Signature of the Mekong River plume in the western South China Sea revealed by radium isotopes

Weifang Chen,[1,2] Qian Liu,[1] Chih-An Huh,[2] Minhan Dai,[1] and Yu-Chun Miao[2]

Received 11 June 2010; revised 15 August 2010; accepted 25 August 2010; published 1 December 2010.

[1] We investigated the distribution of ^{223}Ra, ^{228}Ra, and ^{226}Ra in the surface water of the western South China Sea (SCS) during summer based on a 30 day cruise conducted in August–September 2007. The activities of ^{223}Ra varied from almost undetectable to 0.74 disintegrations per minute (dpm)/100 L, and those of ^{228}Ra varied from 12.2 to 61.5 dpm/100 L. Their spatial distribution was characterized by a jet of high ^{228}Ra (>48 dpm/100 L) and ^{223}Ra (>0.4 dpm/100 L) extending eastward from the Vietnam coast along ~11°N, curling up in the vicinity of 112°E and swirling counterclockwise to form a cyclonic eddy with lower ^{228}Ra (21–25 dpm/100 L) and ^{223}Ra (0.04–0.14 dpm/100 L) at its center. High ^{226}Ra (10–14 dpm/100 L) appeared in the eastward jet and decreased to 6.0–8.5 dpm/100 L along the track of the jet described above. The observed distribution of Ra isotopes was consistent with the pattern of the Southeast Vietnam Offshore Current in the western SCS in summer. The higher radium activities were in all likelihood derived from the Mekong River. Using a simple two-end-member mixing model based on the ^{228}Ra/^{226}Ra activity ratio and salinity, we calculated that approximately 53% of the surface water in the western SCS was originated from the Mekong River diluted water. Note that this estimation should be regarded as an upper limit due to the lack of sampling at its immediate source, the Mekong estuary. The data revealed that more than 2 weeks were required for the transportation of freshened water from the Mekong River's mouth several hundred kilometers to the western SCS.

Citation: Chen, W., Q. Liu, C.-A. Huh, M. Dai, and Y.-C. Miao (2010), Signature of the Mekong River plume in the western South China Sea revealed by radium isotopes, *J. Geophys. Res.*, *115*, C12002, doi:10.1029/2010JC006460.

1. Introduction

[2] River plumes play an important role in the transport and transformation of terrestrial materials in coastal margins [*Dagg et al.*, 2004]. Along plume boundaries, mixing of dissolved riverine and oceanic components and coagulation and settling of particles create fronts, which are often zones of enhanced biological productivity and biogeochemical reactions [*Lohrenz et al.*, 1990]. However, such processes are highly complex and not easy to grasp due to the dynamic and inhomogeneous nature of river plumes. Plumes from some major rivers may extend hundreds of kilometers into the open ocean [*Muller-Karger et al.*, 1988], and are commonly traced by offshore negative salinity and/or positive silica anomalies. However, the salinity signal can be altered by precipitation and evaporation, and the silica signal is sensitive to biological uptake. To circumvent these drawbacks, radium isotopes can be employed [*Moore and Krest*, 2004; *Moore et al.*, 1986; *Moore and Todd*, 1993; *Rutgers van der Loeff et al.*, 2003]. Unlike salinity and silica, the ^{228}Ra/^{226}Ra activity ratio (AR) only changes by decay of ^{228}Ra and mixing. Moreover, using short-lived radium isotopes (^{223}Ra and/or ^{224}Ra), the time scale of transport of a river plume and its mixing with the adjacent coastal water can be further constrained [*Moore and Krest*, 2004; *Moore and Todd*, 1993]. Thus, from a combined use of two or more Ra isotopes, it is possible to characterize better the dispersal of river water.

[3] There are four naturally occurring radium isotopes, that is, ^{223}Ra ($t_{1/2}$ = 11.4 days), ^{224}Ra ($t_{1/2}$ = 3.6 days), ^{228}Ra ($t_{1/2}$ = 5.75 years) and ^{226}Ra ($t_{1/2}$ = 1600 years), which are introduced to a water body through its contact with thorium-bearing sediments. In fresh river water, Ra isotopes are strongly adsorbed on particles and they tend to be desorbed as the ionic strength of the ambient water increases upon estuarine mixing [*Elsinger and Moore*, 1980; *Key et al.*, 1985; *Li et al.*, 1977]. Following the deposition of sediments, Ra isotopes regenerated by Th decay can be released at the sediment-water interface or into the sediment interstitial water. Due to their vast difference in half-lives, ^{223}Ra and ^{224}Ra are continually regenerated and supplied from the estuarine sediments, while ^{226}Ra and ^{228}Ra are regenerated much more slowly [*Moore and Todd*, 1993]. After complete desorption, ^{223}Ra and ^{224}Ra are expected to change with

[1]State Key Laboratory of Marine Environmental Science, Xiamen University, Xiamen, China.
[2]Institute of Earth Sciences, Academia Sinica, Taipei, Taiwan.

0148-0227/10/2010JC006460

mixing and significantly decay during the lifetime of a plume while ^{226}Ra and ^{228}Ra change primarily by mixing with offshore water. Thus Ra isotopes can be used as tracers to study the advection and mixing of river plumes with ocean water after they leave the river/ocean mixing zone [*Moore*, 2000a, 2000b; *Moore and Krest*, 2004; *Moore and Todd*, 1993].

[4] The Mekong River is one of the largest rivers in the world. It empties into the South China Sea (SCS) at ~10°N and 107°E with a mean annual discharge of 470 km^3 [*Dagg et al.*, 2004]. This freshwater discharge changes seasonally, being lowest in May and highest in October [*Mekong River Commission* (*MRC*), 2008], and the plume flows southward in winter and northward in summer in response to the switch in direction of the monsoon winds [*Hu et al.*, 2000]. In contrast with other extensively studied world major river plume systems, such as the Amazon, Changjiang and Mississippi River plumes [*Chen et al.*, 2008; *Dagg et al.*, 2004; *Lohrenz et al.*, 1999; *Smith and DeMaster*, 1996], little is known about the Mekong River plume. This is true both in terms of the plume variability and the associated biogeochemical processes. Previous study has shown that the Mekong River's influence on nitrogen fixation is confined to the upwelling region off Vietnam along a belt stretching ~500 km from the river's mouth [*Voss et al.*, 2006]. In this study, we used the distribution of three radium isotopes (^{223}Ra, ^{228}Ra, ^{226}Ra) to identify the signature of the Mekong River plume in the western SCS. To our knowledge, this is the first time that ^{223}Ra, ^{228}Ra, and ^{226}Ra were determined concurrently at a high spatial resolution in the western SCS. It enabled us to assess the time scale of the transport of the river plume and its mixing with the adjacent coastal and ocean waters.

2. Materials and Methods

2.1. Study Area

[5] The SCS is the largest marginal sea at low latitude in the world. The western SCS can be roughly divided into two parts: the continental shelf and the deep basin. The shelf is narrow and lies roughly west of 109°E. To the south of the western SCS is a region known as the Nansha Archipelago, where many islands and reefs are irregularly distributed. The climate of the western SCS is tropical and is influenced by the seasonal monsoonal cycle. The monsoonal winds are southwesterly in summer (June–September) and northeasterly in winter (November–March), with transitions in spring (April–May) and fall (October to early November). During the summer, surface circulation in the western SCS is characterized by a unique and strong eastward jet, namely the Southeast Vietnam Offshore Current (SVOC) [*Fang et al.*, 2002; *Hu et al.*, 2000]. This eastward jet leaves the coast between 10°N and 12°N and bifurcates in the vicinity of 113°E. The northern branch flows toward the center of the western SCS and forms a cyclonic eddy off the Vietnam coast, while the southern branch turns to the south and forms an anticyclonic eddy centered in the southern SCS. Thus, there exists a dipole mode circulation off the southeast Vietnam coast [*Fang et al.*, 2002; *Shaw et al.*, 1999]. Upwelling off Vietnam occurs during the summer when the southwest monsoon wind prevails, and it can be enhanced by the eastward jet [*Dippner et al.*, 2007; *Fang et al.*, 2002].

2.2. Sampling

[6] The cruise in the western SCS was conducted from 15 August to 14 September 2007 onboard R/V *Dongfanghong-II*. It was divided into two legs (Table 1 and Figure 1b), with the first leg (15–28 August) visiting stations to the north of 13.5°N and the second leg (1–14 September) occupying the area to the south of 13.5°N and SEATS (115.96°E, 18.03°N, a time series station in the SCS). Station TS1 in leg 1 was revisited in leg 2, when it was renamed Station 3YS4.

[7] During the cruise, large-volume (100 L) samples were pumped from ~5 m below the surface into plastic cubitainers onboard. After the sample volume was recorded, the water was passed immediately through a column of MnO_2-coated acrylic fiber (Mn fiber) to quantitatively remove Ra at a flow rate less than 1 L per minute. The surface temperature and salinity were measured using a YSI 6600 sonde (YSI Co.). This set of data was well calibrated with a SBE-21 CTD unit (Sea-Bird Co.).

2.3. Determination of ^{223}Ra With a RaDeCC System

[8] In the shipboard laboratory, each Mn fiber sample was rinsed with Ra-free deionized water, partially dried with a stream of air and then placed in the radium delayed coincidence counter (RaDeCC) following *Moore and Arnold* [1996]. The RaDeCC utilizes the difference in the decay constants of the short-lived Po daughters of ^{219}Rn and ^{220}Rn to identify alpha particles derived from ^{219}Rn and ^{220}Rn decay and hence to determine activities of ^{223}Ra and ^{224}Ra on the Mn fiber [*Giffin et al.*, 1963; *Moore and Arnold*, 1996]. To reduce the effect of ^{224}Ra on the measurement of ^{223}Ra, the samples were recounted for a longer time after 7–10 days. The expected error of ^{223}Ra measurements was 10% [*Moore*, 2008].

[9] Although the RaDeCC system can provide the ^{223}Ra and ^{224}Ra data simultaneously after a sequence of runs, we failed to obtain the ^{224}Ra data due to a shortage of helium (the carrier gas) onboard during the survey for the last transect (transect Y3). When the samples were returned to the shore-based laboratory about 10 days later, ^{224}Ra had decayed too much to allow further analysis.

2.4. Determination of ^{228}Ra and ^{226}Ra by γ-Spectrometry

[10] In a shore-based laboratory, following the procedure of *Moore et al.* [1985], the Mn fiber sample was leached with a mixture of 1 M hydroxylamine hydrochloride and hydrogen peroxide solution at 50°C. Radium isotopes in the solution were coprecipitated with $BaSO_4$ and the precipitate was stored in a small vial for 3 weeks to allow ^{222}Rn to equilibrate with ^{226}Ra. The absolute ^{226}Ra and ^{228}Ra activities of the sample were measured using a well-type germanium detector (ORTEC, GWL-120-15-S). The detector was calibrated by counting reference sources processed from a solution containing known activities of ^{228}Ra and ^{226}Ra. The solution was prepared by dissolution of Congo pitchblende (with ^{238}U and ^{226}Ra in secular equilibrium) and an old Th-nitrate salt (with ^{232}Th and ^{228}Ra in equilibrium). The ^{226}Ra activity in samples was determined from the photon peaks of its daughters: ^{214}Pb (295.22 and 351.99 keV) and ^{214}Bi (609.32 keV) [*Moore*, 1984], whereas the ^{228}Ra activity was measured via the peaks of

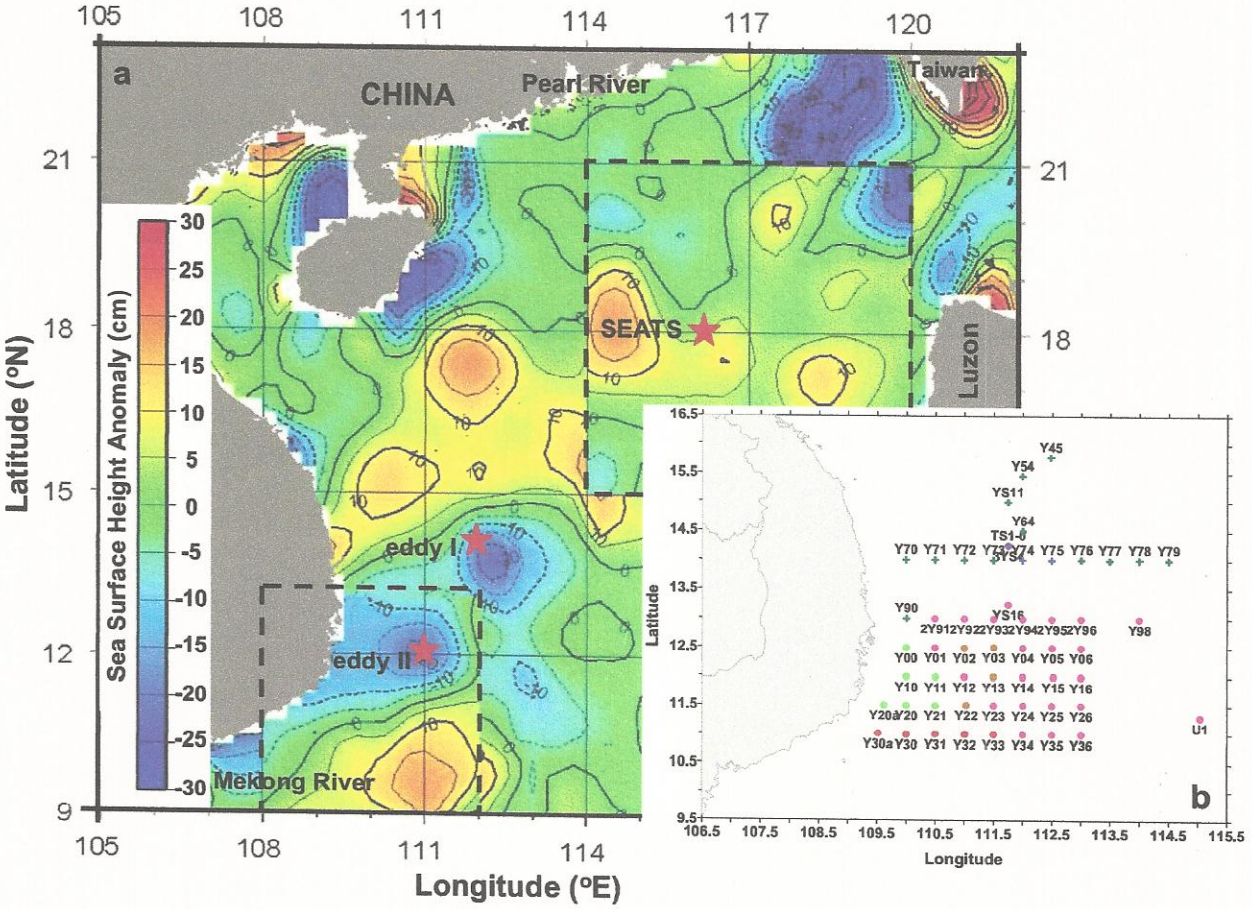

Figure 1. (a) Map showing a mosaic of real-time satellite images (taken on 23 August 2007) with contours of sea surface height anomaly (SSHA) in the South China Sea (http://argo.colorado.edu/~realtime/gsfc_global-real-time_ssh/). The whole image is for 23 August 2007 (date when samples from eddy I were taken), and the dashed lines on the map indicate boundaries of 5 September 2007 (date when samples from eddy II were taken) (108°E to 112°E, 9°N to 13°N) and 13 September 2007 (date when samples from SEATS were taken) (114°E to 120°E, 15°N to 21°N). Against the backdrop of the SSHA are three key stations (indicated by red stars) occupied for this study: eddy I (111.7°E, 14.2°N), eddy II (111.0°E, 12.0°N), and SEATS (115.96°E, 18.03°N). (b) All sampling sites during the cruise. Crosses represent stations during leg 1 (15–28 August 2007), and dots indicate stations in leg 2 (1–9 September 2007). The symbols are shown in various colors (as those used in Figure 4) to distinguish different water masses.

^{228}Ac at 338.63, 911.07 and 968.90 keV [*Elsinger et al.*, 1982; *Moore*, 1984]. The errors for the ^{228}Ra and ^{226}Ra measurements were 5–10%, including counting statistics and standard propagation of errors associated with the data reduction.

3. Results

3.1. Hydrography

[11] During the cruise, two well-developed cold eddies were identified from the sea surface height anomaly (SSHA). These two eddies (referred to as eddy I and eddy II hereafter) were centered at ~112.5°E, 13.5°N and 111°E, 12°N (Figure 1a). Altimetric history of these two cold-core cyclonic eddies suggested the intensification of eddy I from 14 August to 30 August and eddy II from 26 August to 12 September. Two stations were occupied inside the eddies (TS1 in eddy I and Y12 in eddy II; Figure 1b) and sampled during the intensification phases (eddy I: 23 August; eddy II: 5 September; Figure 1a).

[12] Figure 2 shows that sea surface temperature in the area covered varied from 27°C to >30°C and sea surface salinity varied from 31.3 to 34.3. Eddy I, with high salinity (>34) and low temperature (<28°C) at its center, clearly existed around 112°E, 14°N during leg 1 (Figures 2a and 2b), consistent with satellite altimetry observations during the same time showing negative SSHA (Figure 1a).

[13] A strong eastward jet characterized by low salinity (<32) and high temperature (>29°C) leaving the coast of Vietnam around 11°N was observed during leg 2 (Figures 2a and 2b). The low-salinity signal in this area can only be attributed to the input of fresh water from the northward Mekong River plume (J. Y. Hu et al., "The kinematics of a cold eddy in the southwestern South China Sea: An observational study," manuscript in preparation, 2010). *Voss et al.* [2006] have utilized the criterion of S < 33.2 to denote the

Table 1. Radium Isotopes (^{223}Ra, ^{228}Ra, and ^{226}Ra) in the Surface Water of the Western South China Sea

Sample Code	Longitude (°E)	Latitude (°N)	Sampling Date[a]	Salinity	^{223}Ra (dpm 100 L^{-1})	^{228}Ra (dpm 100 L^{-1})	^{226}Ra (dpm 100 L^{-1})	^{228}Ra/^{226}Ra[b]
Y70	110.0	14.0	2007-8-15	33.75	0.02	25.0 ± 8.8	9.0 ± 5.5	2.8 ± 2.0
Y71	110.5	14.0	2007-8-15	33.77	0.05	14.6 ± 2.9	6.4 ± 1.4	2.3 ± 0.7
Y72	111.0	14.0	2007-8-15	33.73	0.06	18.7 ± 3.0	8.8 ± 1.2	2.1 ± 0.4
Y73	111.5	14.0	2007-8-15	33.77	0.01	20.9 ± 2.9	8.4 ± 1.0	2.5 ± 0.5
Y74	112.0	14.0	2007-8-15	34.14	0.07	15.2 ± 1.4	6.6 ± 0.5	2.3 ± 0.3
Y75	112.5	14.0	2007-8-16	34.13	0.01	12.2 ± 2.5	8.6 ± 0.8	1.4 ± 0.3
Y76	113.0	14.0	2007-8-16	33.79	0.01	24.9 ± 1.8	8.1 ± 0.7	3.1 ± 0.3
Y77	113.5	14.0	2007-8-16	33.68	0.03	25.1 ± 3.6	9.5 ± 0.9	2.6 ± 0.5
Y78	114.0	14.0	2007-8-16	33.77	0.04	19.9 ± 2.1	7.5 ± 0.7	2.6 ± 0.4
Y79	114.5	14.0	2007-8-16	33.73	0.02	17.5 ± 2.4	7.8 ± 0.7	2.2 ± 0.4
Y90	110.0	13.0	2007-8-18	33.77	0.07	16.0 ± 1.3	6.2 ± 0.4	2.6 ± 0.3
Y64	112.0	14.5	2007-8-20	33.68	0.02	17.6 ± 1.7	8.0 ± 0.6	2.2 ± 0.3
Y54	112.0	15.5	2007-8-22	33.57	0.01	18.5 ± 2.6	7.2 ± 0.7	2.6 ± 0.4
TS1	111.7	14.2	2007-8-23	34.06	0.00	14.0 ± 1.3	9.4 ± 0.9	1.5 ± 0.2
YS11	111.7	15.0	2007-8-27	33.79	0.13	18.7 ± 1.6	6.7 ± 0.5	2.8 ± 0.3
Y45	112.5	15.8	2007-8-28	33.51	0.18	22.1 ± 2.9	7.5 ± 1.0	3.0 ± 0.5
3YS4	111.8	14.3	2007-9-1	32.63	0.20	48.2 ± 3.1	10.8 ± 0.6	4.5 ± 0.4
YS16	111.7	13.2	2007-9-1	32.46	0.15	45.3 ± 1.8	8.6 ± 0.5	5.3 ± 0.4
2Y91	110.5	13.0	2007-9-2	32.73	0.26	52.5 ± 3.9	11.3 ± 1.0	4.6 ± 0.5
2Y92	111.0	13.0	2007-9-2	33.27	0.13	30.6 ± 2.9	8.0 ± 0.7	3.8 ± 0.5
2Y93	111.5	13.0	2007-9-2	32.79	0.32	46.3 ± 2.9	9.2 ± 0.8	5.1 ± 0.5
2Y94	112.0	13.0	2007-9-3	32.88	0.20	41.4 ± 3.6	11.0 ± 0.8	3.8 ± 0.4
2Y95	112.5	13.0	2007-9-3	33.10	0.05	31.9 ± 3.5	9.1 ± 1.0	3.5 ± 0.5
2Y96	113.0	13.0	2007-9-3	33.27	0.06	24.1 ± 1.9	7.2 ± 0.6	3.4 ± 0.4
Y06	113.0	12.5	2007-9-3	32.66	0.06	28.9 ± 3.8	7.1 ± 1.2	4.1 ± 0.9
Y05	112.5	12.5	2007-9-3	32.83	0.06	32.8 ± 2.5	8.0 ± 1.0	4.1 ± 0.6
Y04	112.0	12.5	2007-9-3	33.04	0.20	28.6 ± 3.2	5.6 ± 1.2	5.1 ± 1.2
Y03	111.5	12.5	2007-9-4	33.23	0.14	24.2 ± 2.2	7.8 ± 0.8	3.1 ± 0.4
Y02	111.0	12.5	2007-9-4	33.49	0.10	24.9 ± 2.5	9.6 ± 1.1	2.6 ± 0.4
Y01	110.5	12.5	2007-9-4	32.93	0.15	37.9 ± 3.2	10.2 ± 2.1	3.7 ± 0.8
Y00	110.0	12.5	2007-9-4	33.70	0.02	15.7 ± 2.0	7.0 ± 1.0	2.2 ± 0.4
Y10	110.0	12.0	2007-9-4	33.70	0.09	16.4 ± 1.6	8.2 ± 1.1	2.2 ± 0.4
Y11	110.5	12.0	2007-9-5	33.42	0.09	18.7 ± 2.0	8.0 ± 0.9	2.3 ± 0.4
Y12	111.0	12.0	2007-9-5	32.59	0.07	35.6 ± 4.2	8.1 ± 1.7	4.4 ± 1.1
Y13	111.5	12.0	2007-9-5	33.53	0.05	21.3 ± 2.3	7.6 ± 0.8	2.8 ± 0.4
Y14	112.0	12.0	2007-9-5	32.41	0.28	46.1 ± 3.6	9.9 ± 1.3	4.7 ± 0.7
Y15	112.5	12.0	2007-9-5	32.26	0.26	38.1 ± 2.9	10.4 ± 0.9	3.7 ± 0.4
Y16	113.0	12.0	2007-9-5	32.38	0.14	42.4 ± 3.6	9.2 ± 1.3	4.6 ± 0.7
Y26	113.0	11.5	2007-9-6	32.41	0.14	39.3 ± 3.3	10.9 ± 1.2	3.6 ± 0.5
Y25	112.5	11.5	2007-9-6	32.38	0.35	31.4 ± 2.2	8.1 ± 0.8	3.9 ± 0.5
Y24	112.0	11.5	2007-9-6	32.51	0.19	36.8 ± 3.2	9.0 ± 1.5	4.1 ± 0.8
Y23	111.5	11.5	2007-9-6	32.53	0.36	36.6 ± 1.9	8.6 ± 0.9	4.2 ± 0.5
Y22	111.0	11.5	2007-9-6	33.43	0.04	22.5 ± 2.8	6.8 ± 0.9	3.3 ± 0.6
Y21	110.5	11.5	2007-9-7	33.60	0.11	16.7 ± 1.8	6.7 ± 0.7	2.5 ± 0.4
Y20	110.0	11.5	2007-9-7	33.72	0.15	14.7 ± 1.9	7.3 ± 0.7	2.0 ± 0.3
Y20a	109.6	11.5	2007-9-7	33.27	0.17	26.0 ± 3.1	7.4 ± 1.1	3.5 ± 0.7
Y30a	109.5	11.0	2007-9-7	31.29	0.54	53.2 ± 2.4	11.5 ± 1.4	4.6 ± 0.6
Y30	110.0	11.0	2007-9-7	31.50	0.46	53.9 ± 4.0	14.0 ± 2.1	3.9 ± 0.6
Y31	110.5	11.0	2007-9-7	31.26	0.74	61.5 ± 2.5	12.8 ± 1.1	4.8 ± 0.5
Y32	111.0	11.0	2007-9-8	31.48	0.57	52.5 ± 2.7	10.3 ± 0.9	5.1 ± 0.5
Y33	111.5	11.0	2007-9-8	31.75	0.41	47.9 ± 2.6	11.6 ± 1.1	4.1 ± 0.5
Y34	112.0	11.0	2007-9-8	32.47	0.17	39.5 ± 4.4	9.5 ± 2.0	4.2 ± 1.0
Y35	112.5	11.0	2007-9-8	32.56	0.04	38.4 ± 2.4	9.9 ± 0.8	3.9 ± 0.4
Y36	113.0	11.0	2007-9-8	32.31	0.34	43.1 ± 3.9	11.7 ± 1.3	3.7 ± 0.5
U1	115.0	11.3	2007-9-8	33.24	0.07	21.9 ± 1.4	6.9 ± 0.5	3.1 ± 0.3
Y98	114.0	13.0	2007-9-9	32.82	0.29	42.4 ± 2.0	9.2 ± 0.9	4.6 ± 0.5

[a]Date format is year-month-day.
[b]Activity ratio.

Mekong River influenced area in the western SCS. Based on the same criterion, our data suggested that the Mekong River may have influenced about half of the western SCS during leg 2 (Figure 2a).

[14] The eastward jet curled up around 112°E and formed a cyclonic eddy centered around 111°E, 12.5°N (eddy II) to the north of the jet, with high-salinity (>33.2) and low-temperature (~28.2°C) water at the center of the eddy (Figures 2a and 2b). Compared to eddy I, the surface signatures of salinity and temperature in eddy II were less evident, which might be due to the Mekong River plume. Hu et al. (manuscript in preparation) suggest that due to surface heating and the Mekong River plume, the surface signatures of eddy II was not as evident as those below 25 m. Such a circulation pattern is again consistent with satellite altimetry observations (Figure 1a) and is also observed in

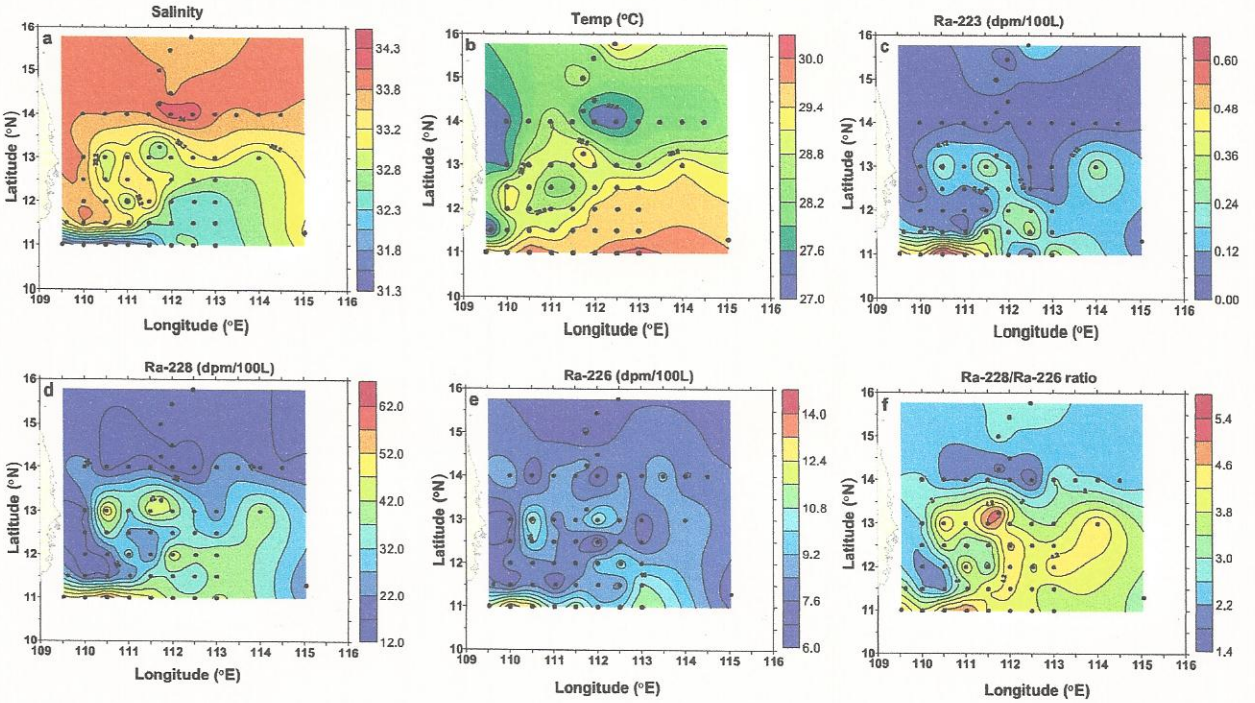

Figure 2. Contour maps showing distribution of (a) salinity, (b) temperature (°C), (c) ^{223}Ra (dpm/100 L), (d) ^{228}Ra (dpm/100 L), (e) ^{226}Ra (dpm/100 L), and (f) ^{228}Ra/^{226}Ra activity ratio in the western South China Sea. Contour lines on the maps are plotted with a software package (SURFERTM by Golden Software) using a linear kriging technique to grid the data points. Note that the contour maps were plotted without considering temporal variations from leg 1 to leg 2 and between stations for the known reasons associated with any ship-based observations.

previous studies [*Fang et al.*, 2002; *Shaw et al.*, 1999], and thus may represent a perennial phenomenon.

[15] Along the southeast Vietnam coast, the elevated salinity (>33.5) suggested upwelling of the subsurface water. As mentioned earlier, coastal upwelling off southeast Vietnam is a typical feature during summer, which is very often enhanced by the eastward jet [*Dippner et al.*, 2007; *Fang et al.*, 2002].

3.2. Water Column Profiles of ^{228}Ra and ^{226}Ra in the SCS

[16] To assess the impact of vertical processes on the distribution of Ra isotopes in surface waters, the water columns at stations TS1 and SEATS were sampled on 23 August and 13 September, respectively, for ^{228}Ra and ^{226}Ra analyses. The profiles (Figure 3) show a sharp decrease with depth of ^{228}Ra across the thermocline and an increase with depth of ^{226}Ra throughout the water column. These trends are typical of these two Ra isotopes and indicate that ^{228}Ra-enriched surface water is advected laterally from adjacent shelf areas, whereas ^{226}Ra is primarily derived from the bottom [*Ku and Luo*, 1994; *Moore*, 1969]. Downward transport of ^{228}Ra is limited by its short half-life and hindered by the strong density gradient below the surface mixed layer. Therefore, ^{228}Ra is usually depleted in the interior of ocean basins and away from boundaries. In contrast, ^{226}Ra is more concentrated near its bottom source, i.e., the ^{230}Th-enriched sediments at the deep ocean floor, and this long-lived Ra isotope can be transported on a basin-wide scale.

[17] These profiles suggested that upwelling of subsurface water lowered ^{228}Ra but raised ^{226}Ra activities at the surface.

3.3. Sea Surface Distribution of ^{223}Ra, ^{228}Ra, ^{226}Ra, and ^{228}Ra/^{226}Ra

[18] Surface activities of ^{228}Ra, ^{226}Ra and ^{223}Ra showed considerable spatial variations in the study area (Table 1 and Figure 2). During leg 1, the ^{223}Ra activity was almost undetectable (<0.1 dpm/100 L) except at Station YS11 and Station Y45, while the ^{228}Ra activity ranged from 12 ~ 25 dpm/100 L with the lowest value around Station TS1 (Figures 2c, 2d, and 2e). We explain this feature by the addition of ^{228}Ra-depleted subsurface water at the center of eddy I.

[19] Ra-223 and Ra-228 measured during leg 2 were higher (>30 dpm/100 L) than those measured during leg 1 except at the center of eddy II and along the Vietnam Coast. The most salient feature during leg 2 was a tongue with high ^{223}Ra (>0.4 dpm/100 L), ^{228}Ra (>48 dpm/100 L) and ^{226}Ra (>10 dpm/100 L) extending eastward from the Vietnam coast along ~11°N (Figures 2c, 2d, and 2e). The presence of the highest ^{223}Ra and ^{228}Ra to the south of the western SCS reaffirmed that the Mekong River was the source of these freshened waters. Along the track of the jet described above,

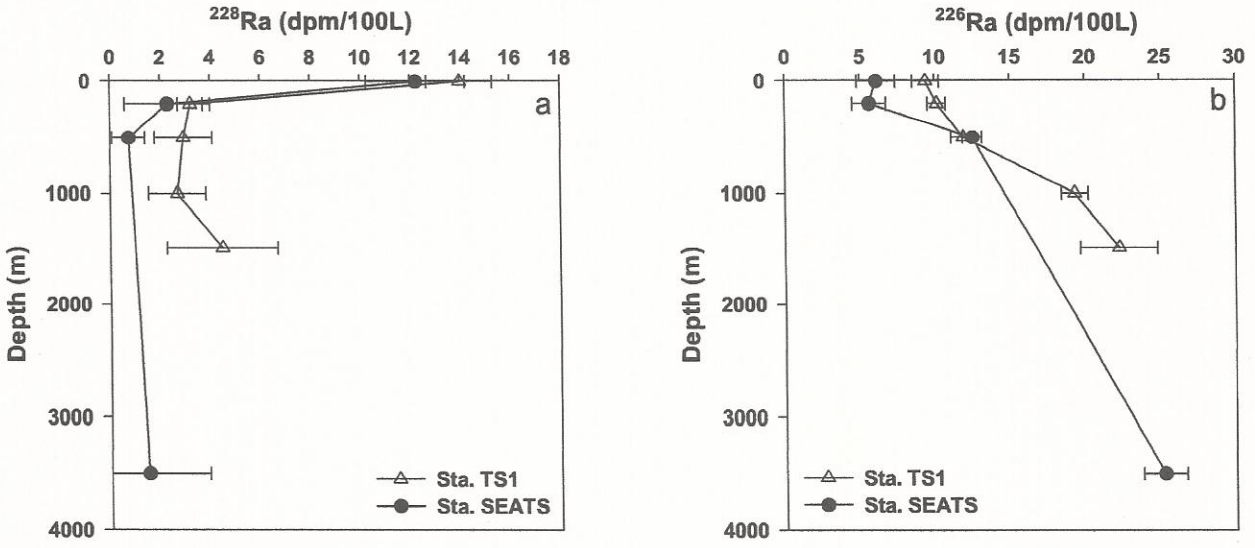

Figure 3. Vertical profiles of (a) ^{228}Ra (dpm/100 L) and (b) ^{226}Ra (dpm/100 L) at Station TS1 (triangles) and Station SEATS (solid circles) in the South China Sea.

the activity of ^{223}Ra decreased from >0.6 to <0.3 dpm/100 L (Figure 2c) due to mixing and radioactive decay. Similar to the pattern of ^{223}Ra, the ^{228}Ra activity decreased from >50 to <30 dpm/100 L along the jet track, mimicking the distribution of salinity (Figure 2d). In contrast, the long-lived ^{226}Ra was more evenly distributed in the western SCS, except in the aforementioned regions with high activities (Figure 2e). Previous studies show that the activity of ^{228}Ra is much higher than that of ^{226}Ra in estuarine waters due to more pronounced release of ^{228}Ra from estuarine sediments [*Key et al.*, 1985; *Moore*, 1981; *Moore et al.*, 1986]. Due to its much longer half-life, the decay of ^{226}Ra can be ignored. Thus the concentration gradient of ^{226}Ra between inshore and offshore waters was much smaller compared with those of ^{223}Ra and ^{228}Ra.

[20] Along the Vietnam coast (stations Y00, Y10, Y20a and Y20), the ^{223}Ra activities were low or almost undetectable (<0.15 dpm/100 L) and the ^{228}Ra activities were also low (averaging 16.8 ± 1.2 dpm/100 L) compared to other sites occupied during leg 2. In view of the location of these sites, coastal upwelling off the southeast Vietnam, which is a typical phenomenon in summer, may be responsible for the observed low activities. Compared to those around the center of eddy I (Station Y74, Station Y75 and Station TS1, 14–16 dpm/100 L) and the aforementioned upwelling regime, ^{228}Ra activities at the center of eddy II were substantially higher (20–25 dpm/100 L). We relate this to the encirclement of the Mekong River plume around the edge of eddy II (Hu et al., manuscript in preparation).

[21] Our ^{228}Ra and ^{226}Ra activities measured during leg 1 compared favorably with those reported previously for adjacent locations in winter (^{228}Ra: 14.9–18.4 dpm/100 L; ^{226}Ra: 7.0–8.7 dpm/100 L) [*Nozaki and Yamamoto*, 2001]. Also, the ^{228}Ra activities measured during leg 2 were comparable with the values in the Nansha Archipelago (i.e., to the south of the eastward jet) in the same season (>30 dpm/100 L) [*Huang et al.*, 1996]. However, in November, the activities of ^{228}Ra in the Nansha Archipelago dropped to 19.6 dpm/100 L [*Cai et al.*, 2002], similar to our results during leg 1. In summer, the eastward jet bifurcates in the vicinity of 113°E with the southern branch turning to the south [*Fang et al.*, 2002; *Shaw et al.*, 1999], which might result in higher ^{228}Ra activities in the Nansha Archipelago during this period.

[22] During leg 1, the ^{228}Ra/^{226}Ra ARs were lowest (1.4–2.3) at the center of eddy I and averaged 2.6 ± 0.3 for the rest of the sites (Figure 2f). In contrast, the ^{228}Ra/^{226}Ra ARs obtained in leg 2 were substantially higher (>3), with the lowest ratios (<2.6) confined to the coastal upwelling area. Along the pathways of the jet, the ^{228}Ra/^{226}Ra ARs were 3.4–5.3, which stood out from the study area and certainly represented water from the Mekong estuary (Figure 2f).

3.4. Radium Isotope Versus Salinity Diagrams

[23] In lieu of T-S diagrams, the ^{228}Ra activities and ^{228}Ra/^{226}Ra ARs were plotted versus salinity to identify water masses in the western SCS (Figures 4a and 4c). The ^{223}Ra and ^{226}Ra activities were also plotted versus salinity for further reference (Figures 4b and 4d). Based on these plots, the surface seawater in the study area may be roughly divided into six water masses, two for leg 1 and four for leg 2 (Which are also indicated in Figure 1b by the same colored symbols as in Figure 4). The former two were set out at the high-salinity end (>33.5) with low ^{228}Ra/^{226}Ra ARs (<3) in Figure 4c while the latter four lay at the opposite end except the coastal upwelling water (CUW). During leg 1, the surface water, apart from eddy I, was not affected by the freshened water and had ^{228}Ra/^{226}Ra ARs similar to the values for winter surface water (~2.2 [*Nozaki and Yamamoto*, 2001]). Thus it represented the surface water under normal "background" conditions. At the center of eddy I, the surface water showed a different characteristic. If the water at 200 m of Station TS1 was used to represent the subsurface water, the plots of ^{228}Ra and ^{228}Ra/^{226}Ra AR versus salinity suggested

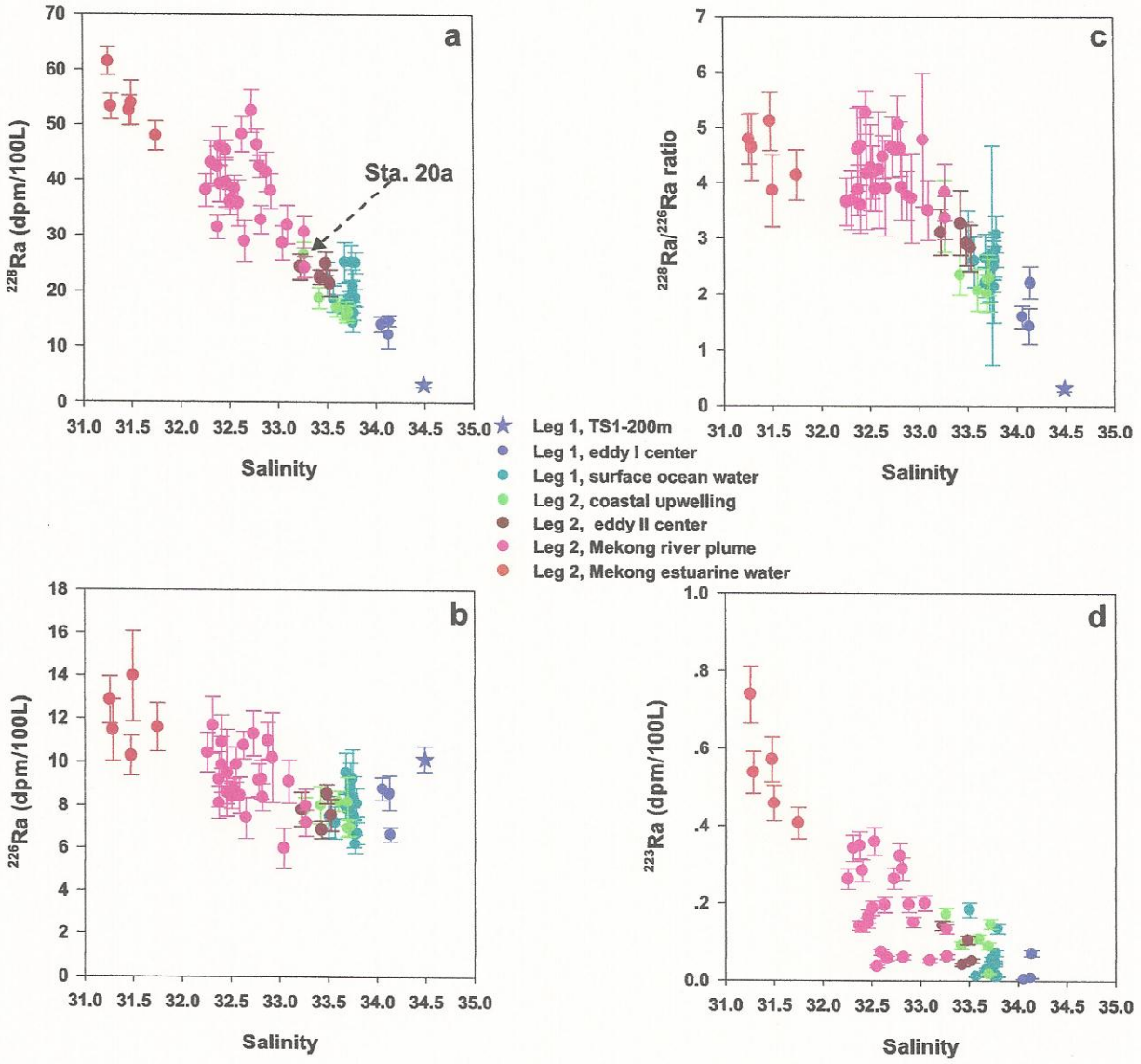

Figure 4. Diagrams of (a) ^{228}Ra (dpm/100 L), (b) ^{226}Ra (dpm/100 L), (c) ^{228}Ra/^{226}Ra, and (d) ^{223}Ra (dpm/100 L) versus salinity in the surface water of the western South China Sea. The water was categorized into six groups: eddy I center water (blue dots), surface ocean water (dark cyan dots), coastal upwelling water (green dots), eddy II center water (dark red dots), Mekong River plume water (pink dots), and Mekong estuarine water (red dots). The blue star represents subsurface water at the center of eddy I.

that the surface water at the center of eddy I was a mixture of the ambient surface water and the subsurface water.

[24] Characterizing the surface water during leg 2 was more complicated. Although it was relatively easy to identify the Mekong estuarine water (S < 32), the water can only be taken as a pseudo-end-member for river water. The other water masses were Mekong River plume water (MRPW), eddy II center water (ECW) and coastal upwelling water (CUW) (Figure 4). The criterion of S < 33.2 and higher ^{228}Ra/^{226}Ra ARs (>3) was used to denote the MRPW. It would be difficult to distinguish between ECW and CUW based on temperature-salinity or silica-salinity relationships (M. Dai, unpublished data, 2007). However, this can be done more easily using the ^{228}Ra and ^{228}Ra/^{226}Ra AR versus salinity diagrams. Unlike the water at the center of eddy I, the ECW was located between the ambient surface water (leg 1) and the MRPW in the diagram (Figure 4c), implying that the latter was swirled into the former and entrained in the eddy. In comparison with the ECW, the CUW was closer to the subsurface water (Figure 4c), suggesting more subsurface water input from coastal upwelling. Thus, higher ^{228}Ra activities and ^{228}Ra/^{226}Ra ARs appeared in the ECW,

making a fine distinction between ECW and CUW. It should be noted that, although the water at Station Y20a was categorized as the CUW, it was somewhat distant from the CUW at other sites but closer to the MRPW in Figure 4a, which suggested that it might be affected by the Mekong River plume or by diffusion of the coastal water for it was inshore of other stations.

4. Discussion

4.1. Revealing the Mekong River Plume Component

[25] The rather high ^{228}Ra activities and ^{228}Ra/^{226}Ra ARs in the western SCS and hence steep gradients of these values clearly showed the influence of the Mekong River plume on the study area. Assuming conservation of salt and the longer-lived radium isotopes (^{228}Ra and ^{226}Ra) and using the two-end-member mixing model of *Moore et al.* [1986] and *Moore and Todd* [1993], the contribution of the Mekong estuary water to the surface water in the western SCS can be estimated by solving the following equations:

$$f_{oc} + f_{es} + f_{P-E} = 1 \quad (1)$$

$$S_{obs} = S_{oc} \times f_{oc} + S_{es} \times f_{es} \quad (2)$$

$$AR_{obs} = \left(^{228}Ra_{oc} \times f_{oc} + ^{228}Ra_{es} \times f_{es}\right) / \left(^{226}Ra_{oc} \times f_{oc} + ^{226}Ra_{es} \times f_{es}\right) \quad (3)$$

where f means the fraction (out of 1), S is salinity, ^{228}Ra and ^{226}Ra are activities of the indicated Ra isotopes, AR is the ^{228}Ra/^{226}Ra activity ratio, and the subscripts oc, es, obs, E and P represent the oceanic end-member, the estuarine end-member, the observed values, evaporation and precipitation, respectively. Here, salinity was used to correct for evaporation/precipitation. Although we can solve the two-end-member mixing model with the ^{226}Ra or the ^{228}Ra distribution alone, it is better to choose the ^{228}Ra/^{226}Ra activity ratio not only for better quality of the activity ratio (determined from one gamma spectrum), but also to reduce the effect of biological utilization of a single isotope on the calculation.

[26] From the above equations, f_{es} and f_{oc} can be solved as follows:

$$f_{es} = \frac{S_{obs} \times (AR_{obs} \times ^{226}Ra_{oc} - ^{228}Ra_{oc})}{AR_{obs} \times (^{226}Ra_{oc} \times S_{es} - ^{226}Ra_{es} \times S_{oc}) - ^{228}Ra_{oc} \times S_{es} + ^{228}Ra_{es} \times S_{oc}} \quad (4)$$

$$f_{oc} = \frac{S_{obs} - S_{es} \times f_{es}}{S_{oc}} \quad (5)$$

[27] In applying the model, there are two underlying assumptions. One is that salinity and the activities of Ra isotopes in the two end-members do not change over the time period of interest; the other is that there is no addition or loss of Ra isotopes except by horizontal mixing [*Moore et al.*, 1986; *Moore and Todd*, 1993]. In our study, the second assumption was obviously not applicable to the coastal upwelling regime due to the input from the subsurface water. Thus, the estuarine fraction was estimated only for the stations covered by the MRPW as defined by the radium isotope versus salinity diagrams. The following end-member values were used in the calculation:

$$S_{es} = 31.26$$

$$^{228}Ra_{es} = 61.5 \pm 2.5 \text{ dpm}/100\text{ L}$$

$$^{226}Ra_{es} = 12.8 \pm 1.1 \text{ dpm}/100\text{ L}$$

$$S_{oc} = 33.74$$

$$^{228}Ra_{oc} = 21.7 \pm 3.3 \text{ dpm}/100\text{ L}$$

$$^{226}Ra_{oc} = 8.5 \pm 0.7 \text{ dpm}/100\text{ L}$$

[28] Here, the values at Station Y31 were taken to represent the estuarine end-member because of the lowest-salinity and the highest ^{228}Ra and ^{223}Ra activities, while the average values for section Y7 during leg 1 were used as the oceanic end-member. However, the values at Station Y74 and Station Y75 were excluded because they were probably influenced by the subsurface water.

[29] The calculated values for f_{es} in the western SCS are listed in Table 2 and Figure 5. To the east of 112°N, the f_{es} values decreased with distance offshore and were less than 50% except at Station Y16 and Station Y98. In contrast, the f_{es} values varied from 40% to 140% to the west of 112°N without any obvious trend, probably suggesting more complicated oceanic conditions in that region. Small-scale irregularity in convergence/divergence associated with an eddy or upwelling might add or subtract Ra isotopes from the system and affect the model calculation. To cancel out these possible effects we took all stations, except the upwelling regime and those affected by eddy II during leg 2, as a whole and calculated an overall f_{es} value of 0.53 based on the same end-member values. It should be noted that any results derived from a model are no better than the assumptions made. In this case, we were not able to test the assumption that the estuarine component remained constant over the time period of interest. Nor could we fully justify our use of the pseudo estuarine end-member. Previous studies show that the calculation of the f_{es} value is very sensitive to the assignment of end-member values [*Moore et al.*, 1986]. We performed a sensitivity analysis of the f_{es} by varying salinity and Ra activities for the estuarine end-member (Figure 6). For initial ^{228}Ra and ^{226}Ra activities (^{228}Ra = 61.5 dpm/100 L; ^{226}Ra = 12.8 dpm/100 L), setting the estuarine end-member at S = 21 rather than S = 31.26 would increase the computed estuarine component by 20%. On the other hand, with salinity fixed, changing either ^{228}Ra or ^{226}Ra activities by ±5% from the values given above would result in changes of the f_{es} value by 10–40%. The

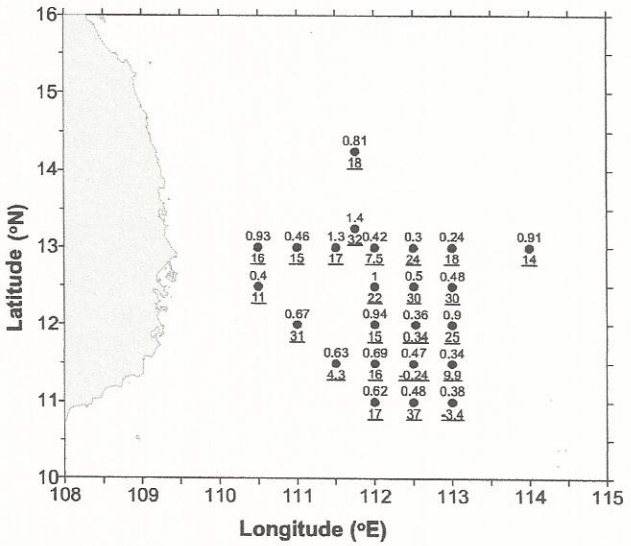

Figure 5. Map showing spatial variation of the estuarine component f_{es} (values indicated above the dots) and apparent age (underlined values below the dots) of the Mekong River plume in the western South China Sea. These values were calculated using a model and with the end-member discussed in the text.

uncertainty of the model and the use of the pseudo estuarine end-member might explain the unusually high f_{es} and negative f_{oc} at some stations. Despite all these uncertainties, the rough estimates made above still revealed a strong signature of the Mekong River plume in the western SCS, although quantitative assessment remains difficult.

4.2. Age of the Mekong Plume Water Derived From ^{223}Ra

[30] The ^{223}Ra-salinity relationship shown in Figure 4d, with the highest ^{223}Ra activity corresponding to the lowest salinity near the Mekong River estuary, unequivocally points to the dispersal of the river water offshore. After this plume water enters the western SCS, it floats at the surface and is carried farther away from the estuarine water and sediment-water interface, i.e., the sources of ^{223}Ra. Thus, the decrease of ^{223}Ra in these waters may be used to estimate the apparent age of the Mekong River plume with reference to its end-member water along its transport pathway. This method was proven to be applicable to the study of the Mississippi plume [*Moore and Krest*, 2004]. The equation for apparent age (t) is

$$t = -\frac{\ln\left[\frac{^{223}Ra_{obs}}{^{223}Ra_{es} \times f_{es}}\right]}{\lambda_{223}} \quad (6)$$

where λ_{223} is the decay constant of ^{223}Ra, 0.061 d^{-1}.

[31] The calculated apparent ages of the MRPW varied from a few days to more than one month, with most of them longer than 10 days (Table 2 and Figure 5). A significant uncertainty in the ^{223}Ra-derived ages is the determination of f_{es}, and therefore the negative water ages might be related to the unusually high f_{es}. Additionally, the initial ^{223}Ra activities might vary temporally in the estuary due to the difference in sediment interaction and groundwater input [*Moore*, 2000a], which could also affect the estimate of ^{223}Ra-derived ages. Using f_{es} = 0.53, $^{223}Ra_{es}$ = 0.74 dpm/100 L (Station Y31) and $^{223}Ra_{obs}$ = 0.167 dpm/100 L (i.e., the average of all stations except the upwelling regime during leg 2), the calculated age was ~14 days. This represented an

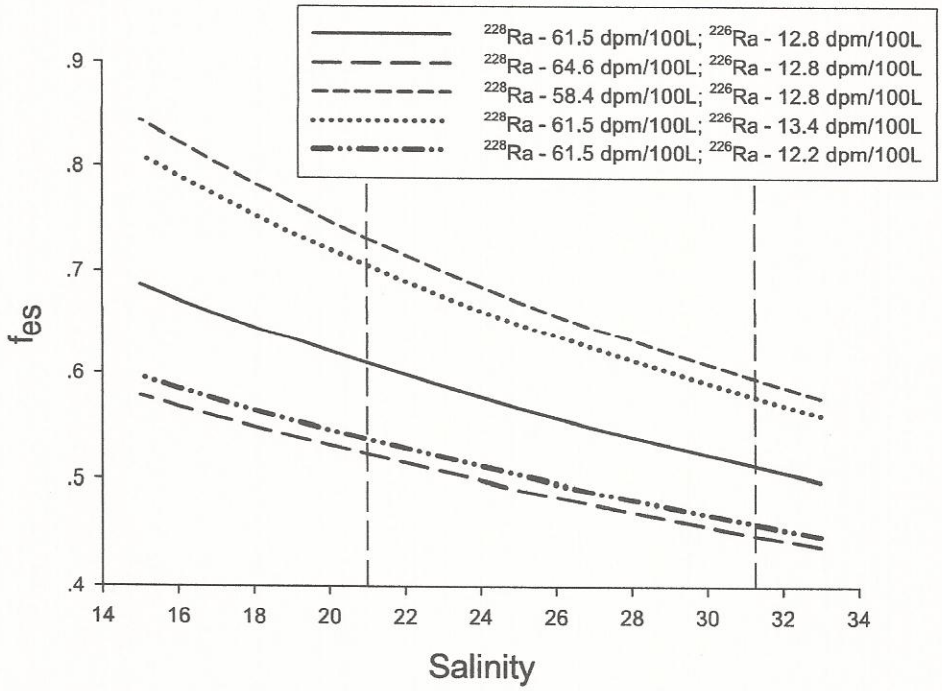

Figure 6. A schematic plot showing the sensitivity of the calculated f_{es} value to the assigned salinity, the initial Ra activities (^{228}Ra = 61.5 dpm/100 L; ^{226}Ra = 12.8 dpm/100 L), and their variations (i.e., ±5%).

Table 2. Values Used on a Two-End-Member Mixing Model and the Calculated Ages of Freshened Waters in the Western South China Sea

	Salinity	$^{228}Ra/^{226}Ra$[a]	^{223}Ra (dpm 100 L^{-1})	Fraction Mekong, End-Member	Age (Days)
Sample 3YS4	32.6	4.5	0.20	0.82	18.3
Sample YS16	32.5	5.3	0.15	1.44	-
Sample 2Y91	32.7	4.6	0.26	0.93	15.6
Sample 2Y92	33.3	3.8	0.13	0.48	16.0
Sample 2Y93	32.8	5.1	0.32	1.25	-
Sample 2Y94	32.9	3.8	0.20	0.44	8.3
Sample 2Y95	33.1	3.5	0.05	0.33	25.4
Sample 2Y96	33.3	3.4	0.06	0.27	19.5
Sample Y06	32.7	3.9	0.06	0.50	30.6
Sample Y05	32.8	3.9	0.06	0.51	30.2
Sample Y04	33.0	4.8	0.20	1.04	21.8
Sample Y01	32.9	3.7	0.15	0.42	11.8
Sample Y12	32.6	4.2	0.07	0.67	31.5
Sample Y14	32.4	4.7	0.28	0.94	14.5
Sample Y15	32.3	3.7	0.26	0.38	1.3
Sample Y16	32.4	4.6	0.14	0.90	25.2
Sample Y26	32.4	3.6	0.14	0.36	11.0
Sample Y25	32.4	3.9	0.35	0.48	0.3
Sample Y24	32.5	4.3	0.19	0.70	16.4
Sample Y23	32.5	4.2	0.36	0.64	4.5
Sample Y34	32.5	4.2	0.17	0.63	16.9
Sample Y35	32.6	3.9	0.04	0.49	37.7
Sample Y36	32.3	3.7	0.34	0.40	−2.5
Sample Y98	32.8	4.6	0.29	0.91	13.8
Average[b]	32.8 ± 0.4	4.0 ± 0.6	0.17 ± 0.10	0.53	13.9

[a]Activity ratio.
[b]The average for the stations except for the coastal upwelling regime during leg 2.

apparent time period for the Mekong plume to travel from the perceived location of the pseudo estuarine end-member (to be further discussed in 4.3).

[32] In addition to ^{223}Ra, ^{224}Ra is also a potential tracer for calculating the apparent age of freshened water. However, ^{224}Ra should be applied to a time scale less than 2 weeks due to its short half-life. For instance, using ^{224}Ra, *Moore and Todd* [1993] calculate an age of less than 10 days for freshened water in the Caribbean Sea and, using $ex^{224}Ra/^{223}Ra$, *Moore and Krest* [2004] obtain an age of <14 days for most of the Mississippi plume water. Considering the long distance from Station Y31 to the Mekong estuary (~10°N, 107°E), the age of the Mekong plume in the western SCS is probably too old for ^{224}Ra to be a suitable tracer in this case.

4.3. Transit Time of the Mekong Plume Water

[33] During the cruise, Station TS1 was occupied twice, first on 23 August (leg 1) and then on 1 September (leg 2). Indeed, during this 9 day time span, large changes were observed at this site, with the ^{228}Ra activity increasing from 15 to 48.2 dpm/100 L, the ^{223}Ra activity from nil to 0.20 dpm/100 L, and the $^{228}Ra/^{226}Ra$ AR from 1.5 to 4.5. Meanwhile, salinity decreased from 34.06 to 32.63 (Table 1). Therefore, these changes strongly suggest an increased input of fresh water from leg 1 to leg 2. Since Station TS1 is located in the center of the western SCS, the Mekong River water carried by the SVOC was the only possible explanation for these low-salinity and high radium isotope signals. This scenario is analogous to what was observed in the western Atlantic where the signal of the Amazon River's water could be traced even to a distance 1500 km from the river's mouth [*Moore et al.*, 1986]. The SVOC current system may transport at a velocity of 50–120 cm/s according to *Fang et al.* [2002]. Using the lower end of the current velocity, it would take ~2 weeks to travel ~700 km, approximately the distance from the Mekong River's mouth to Station TS1. This estimate was consistent with the Mekong plume age derived from ^{223}Ra.

[34] Although we do not have time series data of Ra isotopes in the eddy, surface salinity at TS1 remained high

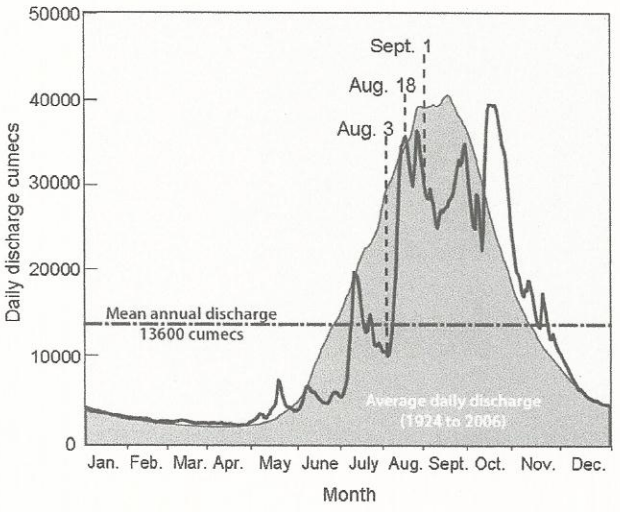

Figure 7. The daily discharge (m^3/s (cumecs)) in 2007 (thick line) compared with an 83 year historical mean daily discharge (thin curve) and mean annual discharge (the dash-dotted line) at Kratie (the lower reach of the Mekong River) (redrawn from Figure 30 of *MRC* [2008] with permission).

from 22 August to 27 August without any indication of freshwater input during this period (M. Dai, unpublished data, 2007). Based on the daily discharge record at Kratie (the lower reaches of the Mekong River), 3 August marked the beginning of the 2007 flood season of this river [*MRC*, 2008] and the first peak discharge happened on 18 August (Figure 7). It is interesting to note that the interval between these dates and the time when Station TS1 was revisited (27 August to 1 September) again supports the view that it may take 2–4 weeks for Mekong River water to reach Station TS1.

5. Conclusion

[35] Isotopes of Ra constitute a unique set of tracers for studying river plumes and the associated water circulation and biogeochemical processes. Their utility as built-in time elements for water in the plume cannot be readily replaced by other means.

[36] During August–September 2007, a jet of water with high radium activities and high $^{228}Ra/^{226}Ra$ ARs extended eastward from the Vietnam coast along ~11°N, curling up in the vicinity of 112°E and swirling counterclockwise to form a cyclonic eddy to the north of the western SCS. In contrast, lower levels of ^{228}Ra and $^{228}Ra/^{226}Ra$ were observed in the coastal upwelling and at the center of cold eddies. The observed distribution of Ra isotopes was consistent with the general circulation pattern of surface water in the western SCS in summer.

[37] The source of the observed high radium activities was no doubt the Mekong River plume. Using a simple two-end-member mixing model based on the $^{228}Ra/^{226}Ra$ AR and salinity, we estimated that approximately 53% of the surface water in the western SCS originated from the Mekong River plume in summer. The apparent age derived from ^{223}Ra revealed that more than 2 weeks were required to transport the freshened water several hundred kilometers from the Mekong River mouth into the western SCS. These estimates entailed the use of a pseudo estuarine end-member (Station Y31) due to difficulties in taking samples in the estuarine mixing zone. Despite the fact that the Mekong estuary was not studied in this work, our data strongly demonstrated the applicability of Ra isotopes in studying water mixing processes after the Mekong River plume left the river mouth. Although they may lead to uncertainties of 10–40% or even more in the calculation of f_{es}, these estimates still reveal a strong signature of the Mekong River plume in the western SCS.

[38] Besides supplying radium isotopes, the river plume may provide nutrients and other materials, thus affecting the biogeochemistry (such as nitrogen fixation) in its estuary and beyond. Further effort is certainly warranted to explore the utility of multiple Ra isotopes in studying the oceanic circulation and mixing of riverine water and the associated chemical dynamics.

[39] **Acknowledgments.** This work was supported by the Natural Science Foundation of China through grant 40821063 and by the NSC through grant NSC97-2611-M-001-002-MY3. We are grateful to the captain and crew of R/V *Dongfanghong-II* for their assistance at sea. We also thank Tzu-Chi Yeh, Qian Li, and Yang Liu for their help in the field and/or in the laboratory and Professor John Hodgkiss for polishing the English in this manuscript. Comments from Michiel Rutgers van der Loeff and an anonymous reviewer have improved the quality of the paper.

References

Cai, P., Y. Huang, M. Chen, L. Guo, G. Liu, and Y. Qiu (2002), New production based on ^{228}Ra-derived nutrient budgets and thorium-estimated POC export at the intercalibration station in the South China Sea, *Deep Sea Res., Part I, 49*, 53–66, doi:10.1016/S0967-0637(01)00040-1.

Chen, C.-T. A., W. Zhai, and M. Dai (2008), Riverine input and air-sea CO_2 exchanges near the Changjiang (Yangtze River) Estuary: Status quo and implication on possible future changes in metabolic status, *Cont. Shelf Res.*, *28*, 1476–1482, doi:10.1016/j.csr.2007.10.013.

Dagg, M., R. Benner, S. Lohrenz, and D. Lawrence (2004), Transformation of dissolved and particulate materials on continental shelves influenced by large rivers: Plume processes, *Cont. Shelf Res.*, *24*, 833–858, doi:10.1016/j.csr.2004.02.003.

Dippner, J. W., K. V. Nguyen, H. Hein, T. Ohde, and N. Loick (2007), Monsoon induced upwelling off the Vietnamese coast, *Ocean Dyn.*, *57*, 46–62, doi:10.1007/s10236-006-0091-0.

Elsinger, R. J., and W. S. Moore (1980), ^{226}Ra behavior in the Pee Dee River–Winyah Bay estuary, *Earth Planet. Sci. Lett.*, *48*, 239–249, doi:10.1016/0012-821X(80)90187-9.

Elsinger, R. J., P. T. King, and W. S. Moore (1982), Radium-224 in natural waters measured by γ-ray spectrometry, *Anal. Chim. Acta*, *144*, 277–281, doi:10.1016/S0003-2670(01)95545-X.

Fang, W., G. Fang, P. Shi, Q. Huang, and Q. Xie (2002), Seasonal structures of upper layer circulation in the southern South China Sea from in situ observations, *J. Geophys. Res.*, *107*(C11), 3202, doi:10.1029/2002JC001343.

Giffin, C., A. Kaufman, and W. Broecker (1963), Delayed coincidence counter for the assay of actinon and thoron, *J. Geophys. Res.*, *68*, 1749–1757, doi:10.1029/JZ068i006p01749.

Hu, J., K. Hiroshi, H. Hong, and Y. Qu (2000), A review on the currents in the South China Sea: Seasonal circulation, South China Sea warm current and Kuroshio intrusion, *J. Oceanogr.*, *56*, 607–624, doi:10.1023/A:1011117531252.

Huang, Y., X. Chen, Y. Xie, D. Jiang, Y. Qiu, F. Chen, and P. Cai (1996), The utility of tracer ^{228}Ra for studying eddy diffusion processes in the Nansha sea area, in *Isotope Marine Chemistry of Nansha Islands Waters* (in Chinese), edited by Multidisciplinary Oceanographic Expedition Team of Chinese Academy of Sciences to the Nansha Islands, pp. 70–78, China Ocean Press, Beijing.

Key, R. M., R. F. Stallard, W. S. Moore, and J. L. Sarmiento (1985), Distribution and flux of ^{226}Ra and ^{228}Ra in the Amazon River Estuary, *J. Geophys. Res.*, *90*, 6995–7004, doi:10.1029/JC090iC04p06995.

Ku, T.-L., and S. Luo (1994), New appraisal of radium 226 as a large-scale oceanic mixing tracer, *J. Geophys. Res.*, *99*, 10,255–10,273, doi:10.1029/94JC00089.

Li, Y. H., G. Mathieu, P. Biscaye, and H. J. Simpson (1977), The flux of ^{226}Ra from estuarine and continental shelf sediments, *Earth Planet. Sci. Lett.*, *37*, 237–241, doi:10.1016/0012-821X(77)90168-6.

Lohrenz, S. E., M. J. Dagg, and T. E. Whitledge (1990), Enhanced primary production at the plume/ocean interface of the Mississippi River, *Cont. Shelf Res.*, *10*, 639–664, doi:10.1016/0278-4343(90)90043-L.

Lohrenz, S. E., G. L. Fahnenstiel, D. G. Redalje, G. A. Lang, M. J. Dagg, T. E. Whitledge, and Q. Dortch (1999), Nutrients, irradiance, and mixing as factors regulating primary production in coastal waters impacted by the Mississippi River plume, *Cont. Shelf Res.*, *19*, 1113–1141, doi:10.1016/S0278-4343(99)00012-6.

Mekong River Commission (MRC) (2008), *Annual Mekong Flood Report 2007*, 86 pp., Vientiane.

Moore, W. S. (1969), Measurement of Ra^{228} and Th^{228} in sea water, *J. Geophys. Res.*, *74*, 694–704, doi:10.1029/JB074i002p00694.

Moore, W. S. (1981), Radium isotopes in the Chesapeake Bay, *Estuarine Coastal Shelf Sci.*, *12*, 713–723, doi:10.1016/S0302-3524(81)80067-9.

Moore, W. S. (1984), Radium isotope measurements using germanium detectors, *Nucl. Instrum. Methods Phys. Res.*, *223*, 407–411, doi:10.1016/0167-5087(84)90683-5.

Moore, W. S. (2000a), Ages of continental shelf waters determined from ^{223}Ra and ^{224}Ra, *J. Geophys. Res.*, *105*, 22,117–22,122, doi:10.1029/1999JC000289.

Moore, W. S. (2000b), Determining coastal mixing rates using radium isotopes, *Cont. Shelf Res.*, *20*, 1993–2007, doi:10.1016/S0278-4343(00)00054-6.

Moore, W. S. (2008), Fifteen years experience in measuring ^{224}Ra and ^{223}Ra by delayed-coincidence counting, *Mar. Chem.*, *109*, 188–197, doi:10.1016/j.marchem.2007.06.015.

Moore, W. S., and R. Arnold (1996), Measurement of ^{223}Ra and ^{224}Ra in coastal waters using a delayed coincidence counter, *J. Geophys. Res.*, *101*, 1321–1329, doi:10.1029/95JC03139.

Moore, W. S., and J. Krest (2004), Distribution of ^{223}Ra and ^{224}Ra in the plumes of the Mississippi and Atchafalaya rivers and the Gulf of Mexico, *Mar. Chem.*, *86*, 105–119, doi:10.1016/j.marchem.2003.10.001.

Moore, W. S., and J. F. Todd (1993), Radium isotopes in the Orinoco Estuary and eastern Caribbean Sea, *J. Geophys. Res.*, *98*, 2233–2244, doi:10.1029/92JC02760.

Moore, W. S., R. M. Key, and J. L. Sarmiento (1985), Techniques for precise mapping of ^{226}Ra and ^{228}Ra in the ocean, *J. Geophys. Res.*, *90*, 6983–6994, doi:10.1029/JC090iC04p06983.

Moore, W. S., J. L. Sarmiento, and R. M. Key (1986), Tracing the Amazon component of surface Atlantic water using ^{228}Ra, salinity and silica, *J. Geophys. Res.*, *91*, 2574–2580, doi:10.1029/JC091iC02p02574.

Muller-Karger, F. E., C. R. McClain, and P. L. Richardson (1988), The dispersal of the Amazon water, *Nature*, *333*, 56–59, doi:10.1038/333056a0.

Nozaki, Y., and Y. Yamamoto (2001), Radium 228 based nitrate fluxes in the eastern Indian Ocean and the South China Sea and a silicon-induced "alkalinity pump" hypothesis, *Global Biogeochem. Cycles*, *15*, 555–567.

Rutgers van der Loeff, M., S. Kuhne, M. Wahsner, H. Holtzen, M. Frank, B. Ekwurzel, M. Mensch, and V. Rachold (2003), ^{228}Ra and ^{226}Ra in the Kara and Laptev seas, *Cont. Shelf Res.*, *23*, 113–124, doi:10.1016/S0278-4343(02)00169-3.

Shaw, P., S. Chao, and L. Fu (1999), Sea surface height variations in the South China Sea from satellite altimetry, *Oceanol. Acta*, *22*, 1–17, doi:10.1016/S0399-1784(99)80028-0.

Smith, J. W. O., and D. J. DeMaster (1996), Phytoplankton biomass and productivity in the Amazon River plume: Correlation with seasonal river discharge, *Cont. Shelf Res.*, *16*, 291–319, doi:10.1016/0278-4343(95)00007-N.

Voss, M., D. Bombar, N. Loick, and J. W. Dippner (2006), Riverine influence on nitrogen fixation in the upwelling region off Vietnam, South China Sea, *Geophys. Res. Lett.*, *33*, L07604, doi:10.1029/2005GL025569.

W. Chen, M. Dai, and Q. Liu, State Key Laboratory of Marine Environmental Science, Xiamen University, Xiamen, 361005, China. (mdai@xmu.edu.cn)

C.-A. Huh and Y.-C. Miao, Institute of Earth Sciences, Academia Sinica, Taipei 11529, Taiwan.

2,3,7,8-Tetrachlorodibenzo-p-Dioxin (TCDD) and 2,3,7,8-Tetrachlorodibenzo-p-Furan (TCDF) In Blue Crabs and American Lobsters from the New York Bight

Thomas J. Belton, Bruce E. Ruppel, Keith Lockwood and Robert T. Mueller

November 12, 1988

Division of Science and Research
New Jersey Department of Environmental Protection
401 East State Street
CN 409
Trenton, New Jersey 08625

ABSTRACT

An investigation of 2,3,7,8-tetrachlorodibenzo-p-dioxin (TCDD) and 2,3,7,8-tetrachloro dibenzo-p-furan (TCDF) bioaccumulation in blue crabs and American lobsters collected from Newark Bay and the New York Bight revealed widespread contamination across the continental shelf. Separate analyses of muscle and hepatopancreas tissue identified the presence of TCDD and TCDF in the latter tissue only. Analyses of the edible tissue (combined muscle and hepatopancreas) displayed varying concentrations across the ranges of both organisms. Blue crabs from the winter dredge fishery area, at their seaward migratory limit, displayed the highest levels (TCDD = 73 pg./g; TCDF = 67 pg./g). American lobsters sampled beyond the ocean dumpsites for harbor dredge spoils have slightly higher levels of TCDD (Mean: 40 pg./g) than inshore, Ambrose fishery lobsters (31 pg./g) and offshore lobsters caught near the edge of the continental shelf. Some locational differences are caused by offshore dumping of dredge spoils and are shown to fluctuate seasonally due to the migratory movements of the lobsters. The additive toxicity of TCDF was calculated as TCDD equivalents, summed with the measured TCDD and compared to FDA "Levels of Concern" and revealed unacceptable levels of risk associated with the consumption of these organisms.

INTRODUCTION

In 1984, dioxin contamination of soils was discovered at a pesticide-manufacturing site on the Passaic River in New Jersey prompting a study of sediments and biota both upstream to the head of tide and downstream into Newark Bay and the New York Bight (1). Sixty percent of the sediments sampled from the river, adjacent to the facility, showed detectable levels of 2,3,7,8-tetrachloro dibenzo-p-dioxin (TCDD) with higher levels being found upstream and at depth possibly due to the flood dominated, salt--wedge dynamics in the estuary. It is estimated that substantial quantities of this contaminant are in storage within the sediments of the river and its downstream embayment as well as at the dredge spoil dumpsite, 12 miles offshore, in the New York Bight (Figure 1).

A wide range of finfish and crustacea from the river showed tissue levels of TCDD (Figure 1a). Blue crabs from the lower estuary contained the highest concentrations (Mean: 468 pg./g in hepatopancreas and 22 pg./g in muscle). Several migratory species, blue crabs and striped bass from the downstream embayments and American lobsters from nearshore ocean waters also showed elevated levels of TCDD. American lobsters from the New York Bight showed consistently high levels of TCDD in the edible hepatopancreas (Mean: 77 pg./g) and combined muscle and hepatopancreas (Mean: 44 pg./g). These lobsters were collected at the mouth of New York harbor and approximately twenty miles offshore beyond the ocean waste disposal sites for dredge spoils, fly ash and sewage sludge.

The identification of TCDD in blue crabs and lobsters distant from the only apparent source suggested a more widespread zone of contamination and a potentially higher human health risk due to the intensive amount of commercial fishing in these offshore waters. The objectives of the present study were to: 1.) Investigate other potential areas of TCDD impact by sampling the seaward migratory limit of the blue crab (i.e., Raritan Bay) and the entire migratory range of the American lobster within the New York Bight (i.e., up to 150 miles offshore); 2.) Estimate the relative effects of location and season on lobster contamination due to their migratory behavior; 3.) Identify the presence of TCDF in the animals (which shows an equivalent level of toxicity compared to TCDD); 4.) Convert any levels of TCDF found into TCDD equivalents for summation of the total risk as compared to the Food and Drug Administration's (FDA) "Levels of Concern" for TCDD; and to 5.) Investigate the relative role of the Historical Area

Remediation Site (HARS) or ocean dredge material dumpsite as a possible intermediary in the transport of TCDD and TCDF to ocean waters and biota.

EXPERIMENTAL SECTION

Sampling

Blue crabs were collected by the use of crab pots, otter trawls and purchases from commercial Crabbers. Sites sampled included locations from Raritan Bay, Sandy Hook Bay and upper New York harbor. American lobsters were collected in lobster pots and otter trawls for Raritan and Sandy Hook Bays or purchased from commercial lobstermen for deepwater areas. Lobster catch locations were sub-divided into three fisheries as defined by NMFS, the National Marine Fishery Service (2), which generally reflect different ports of departure for the fishing fleets operating in these waters (Figure 2). The Ambrose fishery includes Raritan and Sandy Hook Bays extending to a hypothetical 7 nautical mile radius on the Ambrose Light leading into New York Harbor. This area also includes the blue crab sampling locations previously mentioned. The Alongshore fishery is a box-like area extending from Long Branch to Point Pleasant and extends offshore approximately 25 nautical miles following the Hudson Canyon. This area includes the ocean waste disposal sites for dredge spoils, fly ash and sewage sludge (Note: this sewage sludge dump is now closed and material is now deposited 106 miles offshore). The Offshore fishery extends eastward from the 50-fathom line to the 100-fathom line approximately 100 miles seaward to the edge of the continental shelf.

Analysis

Samples for analysis consisted of standardized edible portions (Figure 2a) including the thoracic, claw, leg and tail meat as well as the hepatopancreas combined (i.e., worst case exposure). Tissue from five organisms of similar size and weight were composited and homogenized in a food processor to generate comparable amounts of material which was then held frozen until extraction. In order to determine if differential bioaccumulation was occurring, a small number of analyses were performed on single lobsters in which the muscle and hepatopancreas tissue were processed separately (Figure 2b).

Tissue analyses were performed using a modified EPA method (3) with high-resolution gas chromatography, low-resolution mass spectroscopy. The modification included a saponification of the tissue prior to the initial extraction. Clean up involved passing the extract through a series of five columns with the final step involving an activated carbopak/elite mix in a 2-cm column with final TCDD and TCDF elution by toluene. Before clean up the samples were fortified with C_{13} labeled TCDD and TCDF as an internal standard. The extracts were analyzed using an electron impact GC/MS instrument with a direct capillary interface, and a 60-meter isomer specific fused silica capillary column. If TCDD or TCDF were not detected, a detection limit was calculated based on a 2.5 times signal-to-noise ratio at the retention time of the respective contaminant and the C_{13} labeled internal standard.

The QA/QC procedures followed EPA guidelines (4) and included spiking tissue of each species with appropriate standards, analyzing replicate and blind control samples and demonstrating the proper isomer specificity and ion ratios. The mean percent recovery for spiked samples with internal standards was 96.8 % with +/- 1 % error for the full range of analyses. The actual values reported in the tables are not corrected for recovery.

Statistics

All data are reported as arithmetic means with the method detection limit of 10 pg./g used for all non-detectable values in summation and statistical analyses. Since it is not possible to catch lobsters at all locations and seasons due to life history characteristics and sampling limitations, it proved difficult to test the significance of any space/time interactions on a strictly monthly or seasonal basis. Knowing that the animals do perform a regular onshore/offshore migration, however, it was possible to separate the data into Spring-Summer (Onshore) and Fall-Winter (Offshore) migration periods. These spatio/temporal differences were tested for significance via a 2-Way ANOVA (5) for unbalanced design on raw and ranked (i.e., non-parametric) data. The model used Season and Location as classes and TCDD and TCDF as the dependent variables. A significance level of 0.05 was used for all hypothesis testing concerning the F statistic.

The data for TCDF was converted to "TCDD Equivalents" via the EPA Toxic Equivalency Factor Method (6) recommended to quantify the additive risk from this contaminant. The results were then compared to the FDA recommended "Levels of Concern" for TCDD in order to estimate the level of unacceptable risk (7). These recommendations are: 1.) No consumption for levels greater than 50 pg./g; and 2.) Reduced consumption for levels between 25 and 50 pg./g.

RESULTS

Blue Crabs

Blue Crabs tissue (i.e., muscle and hepatopancreas combined) from Raritan Bay and the lower Hudson River (Table 1) show mean TCDD concentrations of 73 pg./g (Range 10-260 pg./g) and TCDF at 67 pg./g (Range: 10-110 pg./g). When TCDF is converted to TCDD equivalents the actual concentration increases to 80 pg./g. A large percentage of the captured animals tested positive for both TCDD (53%) and 2,3,7,8-TCDF (73%) with the latter being more ubiquitous. An analysis of the distribution of TCDD and TCDF in Blue Crabs across the harbor (Figure 3) shows that the contaminants are usually found together and an apparent increase in concentration occurs from inner Raritan Bay out to the mouth of the Hudson River. All of the control samples from Delaware Bay showed no detectable levels for either contaminant. The TCDD levels for these Blue Crabs collected in 1986 (at the seaward limit of their migratory range) were similar to levels found (1) within Newark Bay in 1983 (Figure 3a).

American Lobsters

Separate analyses of lobster muscle and hepatopancreas showed that both of the contaminants were present only in the hepatopancreas (Range: TCDD= <10-290 pg./g; TCDF= <10-320 pg./g). However, they may be present at levels below the relatively high detection limits in this study. Analyses of combined muscle and hepatopancreas for the entire New York Bight lobster fishery (Table 1) show mean TCDD concentrations of 28 pg./g (Range: <10-110 pg./g) and TCDF at 26 pg./g (Range: <10-120 pg./g). When TCDF is converted to TCDD equivalents the actual dosage increases to 30 pg./g. In contrast to the crab data, a smaller percentage of the lobsters tested positive for both TCDD (36%) and TCDF (20%) with the former being more ubiquitous. This may reflect the more remote exposure to the source of contamination (Passaic River) or may be due to the large number of lobster analyses showing high detection limits (i.e., >25 pg./g).

If the New York Bight lobster results are broken into sub-fisheries extending progressively offshore as categorized by NMFS (2) the data reveal some significant locational differences (Figure 4). TCDD and TCDF are high in both the Ambrose and Alongshore fisheries but low to non-detectable in the far offshore areas (Figure 4a). The 15 pg./g TCDD for Offshore lobsters is based on only 2 positive results out of 17

composites. The results illustrate that levels of TCDF appear to drop off linearly as one progresses offshore. However, this differs dramatically from the TCDD levels, which are higher in the Alongshore area, near the dredge spoil dumpsite, than in either, the Ambrose or Offshore fishery areas. These spatial differences may be related to seasonal feeding patterns and migratory movements.

In Figure 5a the monthly lobster landings for New Jersey waters (N.J. Div. Fish, Game and Wildlife) are superimposed on the mean monthly TCDD results from the 1985-1986 sampling season. The annual commercial landings appear unimodal. They begin to increase in early spring (March) as water temperatures increase and the lobsters become more active and begin their shoreward migration. The commercial fishing activities also increase at this time, as the lobsters are actively feeding and the milder weather conditions are more suitable to commercial lobstering. The landings reach a peak in late summer (August) and steadily decline thereafter as the water temperature drop and the animals seek deeper water to avoid severe winter conditions.

In contrast the TCDD data for the New York Bight fishery appears bimodal with high values in the winter/early spring followed by a steady rise in contamination from May through September. The latter trend probably reflects the lobster's active feeding and growing phase but does not explain the high levels found in the winter and early spring. These anomalies results become less contradictory if the data are separated into Ambrose and Alongshore areas and examined with an understanding of the seasonal, migrational movements of the lobsters within these sub-fisheries.

The Ambrose lobsters (Figure 5b) consistently had non-detectable levels of TCDD through the spring and summer but then rose remarkably high in the fall and winter. The Alongshore lobsters on the other hand (Figure 5c) had elevated levels of dioxin in all four seasons with an apparent increase in late fall. These trends were similar for both the 1985 and 1986 samplings seasons.

Spatial partitioning for TCDD (Figure 4) originally indicated that levels were higher in the Alongshore than in the Ambrose fishery. Migrational analysis (Figure 6a) reveals that this relationship only holds for the Spring-Summer (onshore migration) period and that by the Fall-Winter (offshore migration) this trend is reversed with higher levels inshore and progressively lower values as sampling moved offshore. Spatial partitioning for TCDF (Figure 4) originally indicated that the highest concentrations were found inshore and that progressively lower levels occurred offshore. Migrational results (Figure 6b) reveal that this relationship only holds for the Fall-Winter (offshore) period and that by the Spring-Summer (onshore migration) the data resemble the TCDD results with higher levels of contamination Alongshore than in the Ambrose fishery. Therefore, on a seasonal/migratory basis the levels and distribution of these two contaminants seem to fluctuate in a similar pattern.

This relationship is borne out statistically by the ANOVA which shows significant differences between location and seasonal effects on the concentrations of both TCDD ($P > F = 0.001^*$) and TCDF ($P > F = 0.03^*$) in American lobsters. Significance results were identical for both raw and ranked data so only the raw results are reported here. However, when the variances are partitioned into a partial sum of squares, season becomes non-significant for TCDD while location ($P > F = 0.02^*$) and the interaction term ($P > F = 0.003^*$) remain significant. The levels of TCDF on the other hand show non-significant effects in the partial sum of squares for location, season and the interaction term.

DISCUSSION

The Blue Crab has only a three year life span which begins as a microscopic larva that is spawned into the nearshore ocean waters. They then undergo a series of sequential metamorphoses, molts and movements back into the estuary where they exist as adults until the females once again migrate seaward to spawn (8). Therefore the animals that were found contaminated in Raritan Bay in 1986 had just entered the estuary from their offshore planktonic stage when the original 1983 investigation was initiated. This indicates that the contamination is not only transported out of the estuary into the nearshore food chain but that it is persistent over time. In addition the amount of TCDD found in these crabs exceeds the FDA's "Level of Concern" recommending no consumption (i.e., >50 pg./g). The presence of TCDF also adds to the risk as indicated by its conversion to TCDD equivalents.

American lobsters in the New York Bight exhibit high yet varying levels of both TCDD and TCDF across their entire geographic range. Although low levels of TCDF congeners have been reported for American lobster hepatopancreas in the past (9) this was the first evidence of TCDD and high TCDF contamination. In addition, the broad distribution of contamination across the New York Bight appears unique compared to other reported contamination events for this species which tend to be localized in the nearshore (10) or estuarine areas (11).

The statistical analysis supports the presence of spatio/temporal differences in TCDD and TCDF contamination in American Lobsters across the New York Bight section of the continental shelf. The lack of significance for TCDF in the partial sum of squares analysis may be due to the unbalanced design and large variances inherent in the data. For TCDD the partitioning analysis indicates that location is more important than season although the significant interaction term suggests that the spatial effects are strongly dependent on the time of year in some unspecified way. Biologically the interaction term may be synonymous with the definition of migratory behavior, which manifests itself as changes in spatial relationships based on temporal cues during the annual life cycle of an organism.

The significance of the location effect and the interaction term may be better understood if we ignore the three artificial fishery boundaries and consider the lobsters as biological populations. Field studies indicate that regardless of latitude the seaward American lobster populations for the eastern continental shelf consist of two sub-populations (12); one that remains in the nearshore area and moves at most 15 km across a home territory and a second deepwater population that resides much further offshore and performs true long-range migration. The seasonal migration is possibly associated with maximizing degree-days for molting, growth, gonadal development, and egg extrusion (13). In addition, the mature lobsters on average move significantly greater distances than immature lobsters with the latter tending to travel along the coastline whereas the larger more mature animals move seaward and to greater depths, as they grow older.

Therefore, the Ambrose and Alongshore locations may circumscribe two ends of the same inshore lobster territory with a size-stratified population moving to variable directions and depths and being exposed alternately to two sources of contamination - the Hudson River plume and the HARS (i.e., ocean dredge spoil disposal site). Moving slowly inshore during the spring/summer period the deepwater, more mature lobsters will mix with the smaller inshore population. Animals in the entire Ambrose fishery then bio-accumulate higher levels of TCDD and TCDF during this more active phase until the mature animals move offshore in the Fall. Then they either depurate some levels during over-wintering at the Alongshore area and/or mix with the landward edge of the less contaminated offshore population resulting in lower

average levels over the winter. In contrast smaller lobsters within the Ambrose fishery aestivate during the winter by burying themselves in the soft muddy channels which criss-cross the Lower Bay. During this time they metabolize much of their stored fat and may release any associated contaminants.

Although it is difficult to separate out the proximate causes of the observed spatio/temporal variations in TCDD and TCDF contamination, we can assume that it includes differences in source exposure, activity cycles, lipid metabolism and possibly depuration. The seasonally persistent high levels of contamination at the seaward end of the inshore population's range (i.e., the Alongshore area) strongly suggests that dredge spoils were supplying a continuous source of TCDD and TCDF to American lobsters. In support of this observation is data from a subsequent study of Newark Bay blue crabs, Alongshore lobsters and soils from the manufacturing site on the Passaic River (14) which reveals similar GC/MS fingerprints of other dioxin and furan congeners between animals and sites.

The amount of TCDD in the New York Bight fishery and more specifically the inshore Ambrose and Alongshore fisheries exceeds the FDA's "Level of Concern" recommending reduced consumption (i.e., >25 pg./g). If TCDF is converted to TCDD equivalents the actual dosage increases in the Alongshore fishery towards a recommendation of no consumption. The large number of lobster analyses showing high detection limits (i.e., 28 % >25 pg./g) may also mask more contamination. This is especially critical when an advisory level exists in the low parts per trillion range. Unfortunately this is a common analytical problem for tissue samples requiring picogram per gram sensitivity since the presence of other organochloride contaminants such as PCBs may mask the presence of both TCDD and TCDF (15). PCBs are a common contaminant in lobsters along the entire eastern seaboard including the New York Bight (1) Long Island Sound (16) and New Bedford Harbor (11). In addition, the conversion to TCDD Equivalents of the other PCDD and PCDF congeners recently found to bioaccumulate in these animals (14) reveals a much higher level of risk than expected from the TCDD and TCDF analysis presented here, although most of the risk comes from the highly toxics TCDD and TCDF.

Concerning the safety of New York Bight lobsters as a food source it is apparent that a threat does exist but the presence of the contaminants in a secondary part of the edible tissue (hepatopancreas) gives health officials some latitude in advising the public concerning the risks. The risk to consumers could be much reduced by not eating the hepatopancreas. I addition, separating the hepatopancreas before cooking (i.e., cooking lyses the organ and disseminates the contamination (10)) can significantly reduce the potential exposure to this contaminant. In addition a recent study has shown that TCDD residues in fish may be reduced through selective cooking and processing techniques (17). A similar study is needed to address the way that lobsters and crabs are usually cooked (i.e., boiled whole). It is to our benefit, considering the Earth's dwindling natural resources, and its ever-increasing human population, to preserve and protect these important food species.

REFERENCES

1. Belton, T.J., Hazen, R., Ruppel, B., Lockwood, K., Mueller, R., Stevenson, E. and J.J. Post, "A Study of Dioxin (TCDD) Contamination in Select Finfish, Crustaceans and Sediments of New Jersey Waterways", N.J. Department of Environmental Protection, Technical Report (1985).

2. Andrews, W.D., "Management of the Lobster, Homarus americanus, Resources of the Continental Shelf, Canyons and Slopes of the Northern Portion of Area IV and Southern Portion of Area III", N.J. Department of Environmental Protection, Technical Report (1980).

3. U.S. Environmental Protection Agency, " Determination of TCDD in Soil and Sediment" EPA Region VII, Kansas City, Technical Report (1983).

4. U.S. Environmental Protection Agency, " Handbook for Analytical Quality Control in Water and Wastewater Laboratories", EPA-600/479-019, (1979).

5. SAS User's Guide: Statistics, Version Five Edition, Cary, N.C., SAS Institute Inc., 956 pp. (1985).

6. Barnes, D.G., Bellin, J. and D, Cleverly, Chemosphere, 15, 1895 (1986).

7. U.S. Food and Drug Administration, " Correspondence from FDA Commissioner Dr. Arthur Hull Hayes Jr. to Governor Milliken Of Michigan concerning advice on the public health significance of TCDD contaminant "Levels of Concern" for finfish in the Great Lakes", August 26, 1981, (1981).

8. Williams, A.B. and T.W. Duke,; in "Pollution Ecology of Estuarine Invertebrates" eds. Hart, C.W. and S.L.H. Fuller, Academic Press, New York, 171-233 (1979).

9. Clement, R.E., Tosine, H.M., Taguchi, V., Musial, C.J. and J. F. Uthe, Bull. Environ. Contam. Toxicol., 39, 1069, (1987).

10. Uthe, J.F., Chou, C.L., Loring, D.H., Rantala,T.T., Bewers, J.M., Dalziel, J., Yeats, P.A. and R. Levaque Charron, Marine Pollution Bulletin, 17, 118, (1986).

11. Weaver, G., Environ. Sci. Technol., 18, 22 (1984).

12. Tracey, M. L., Nelson, K., Hedgecock, D., Shleser, R. A. and M. L. Pressick, J. Fish. Res. Board Can., 32, 2091 (1975).

13. Campbell, A. and A.B. Stasko, Marine Biology, 92, 393 (1986).

14. Rappe, C., Belton, T.J., Bergquist, P., Ruppel, B., Swanson, S. and K. Lockwood, "Levels and Patterns of PCDD abd PCDF Contamination in Fish, Crabs and Lobsters from Newark Bay and the New York Bight", (Manuscript in Preparation)

15. Rappe, C., Enviro. Sci. Technol., 18, 78 (1984).

16. Chytalo, K., New York Department of Environmental Conservation, "Personal Communication".

17. Stachiw, N.C., Zabik, M.E., Booren, A.M. and M.J. Zabik, Jrnl. Agric. and Food Chem., 36, 848, (1988).

Table 1. TCDD, TCDF and TCDD Equivalent[1] Levels in Blue Crabs and American Lobster From Raritan Bay and the New York Bight

Blue Crab	X	TCDD[2] S.D.	n	%Pos	% > 25pg/g4	X	TCDF S.D.	n	% Pos	TCDD Equivalents X
	73.1	(82.9)	15	53	60	70	(36.4)	15	73	80
American Lobster[3]										
New York Bight	27.5	(25.7)	47	36	36	26	(28.9)	39	20	30
Ambrose	31.2	(30.2)	19	37	37	35.0	(35.0)	19	37	34.7
Alongshore	40.5	(22.8)	11	73	73	24.5	(19.5)	11	36	42.9
Offshore	15.0	(13.9)	17	12	12	<10	-	9	0	15.0

1. After Barnes et al 1986
2. Arithmetic means include all non-detectable values at 10 pg/g method detection limit for summation SD = standard deviation N = no of 5 organism composites analyzed % Pos = Percent Positive
3. Lobsters data presented for NY Bight as a whole and its sub-fisheries 4. FDA "Level of Concern" recommending reduced consumption is 25 pg/g

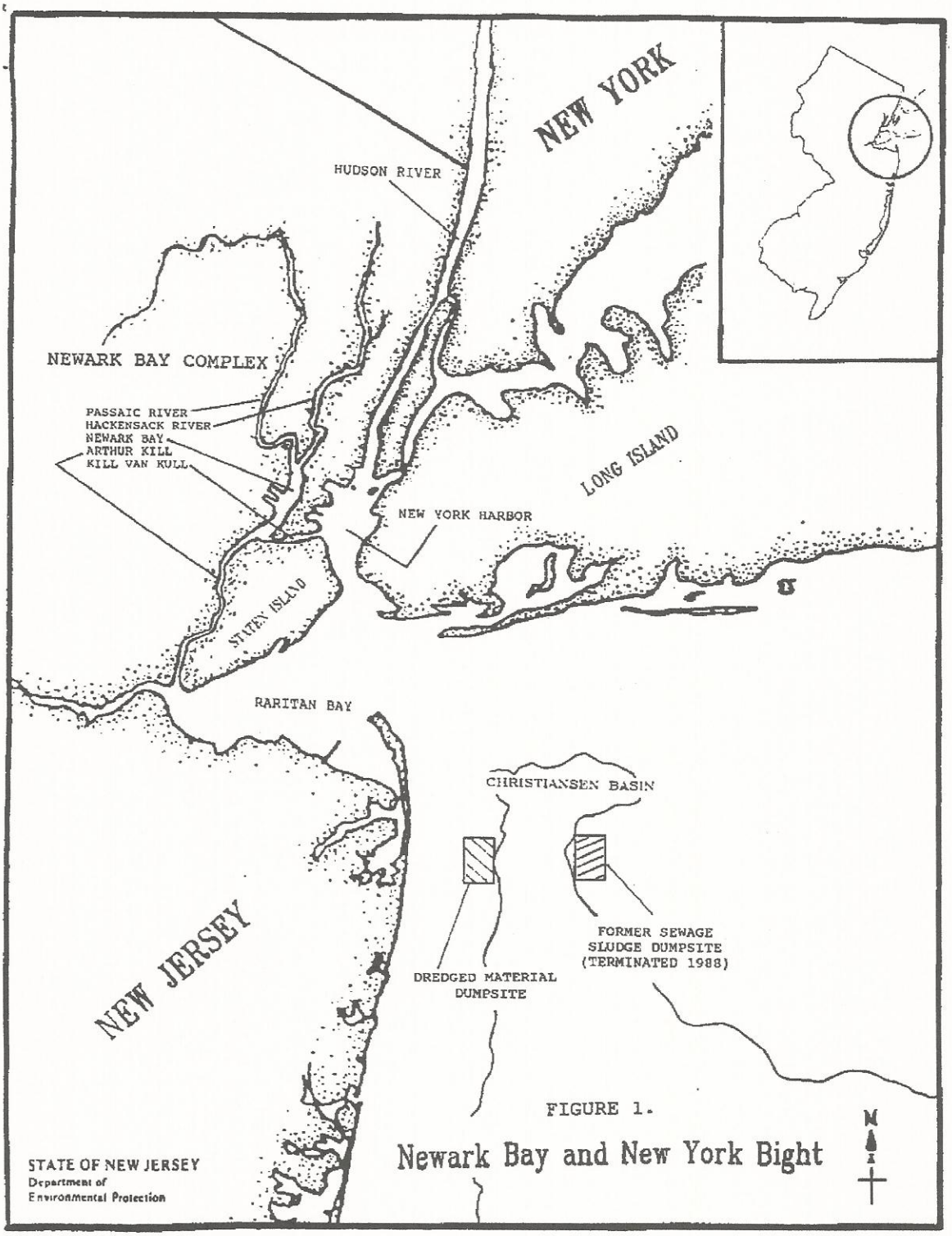

FIGURE 1.

Newark Bay and New York Bight

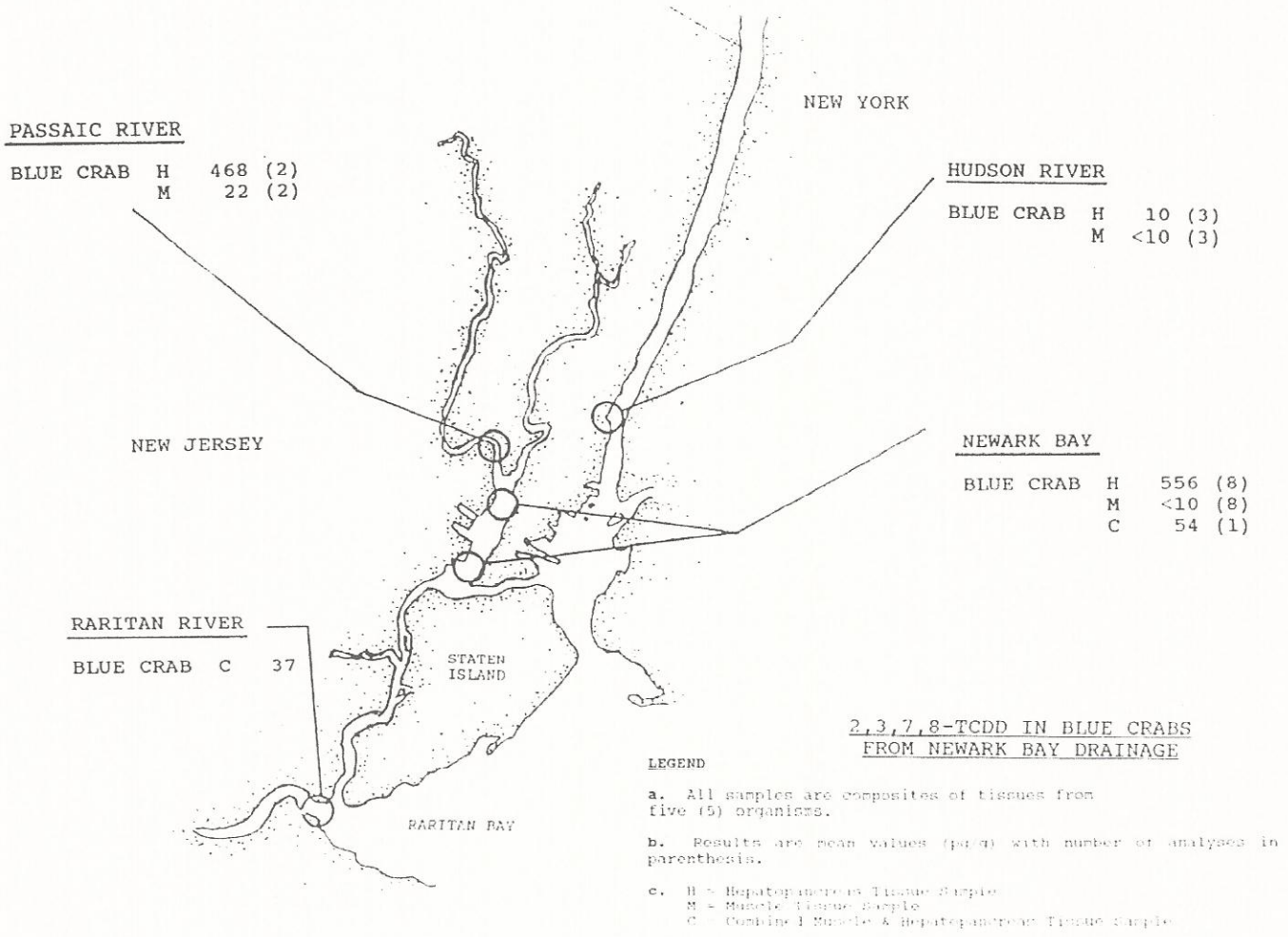

Figure 1a. Dioxin (2,3,7,8,-TCDD) in Blue Crabs From Newark Bay 1984*

From Belton et al. 1985

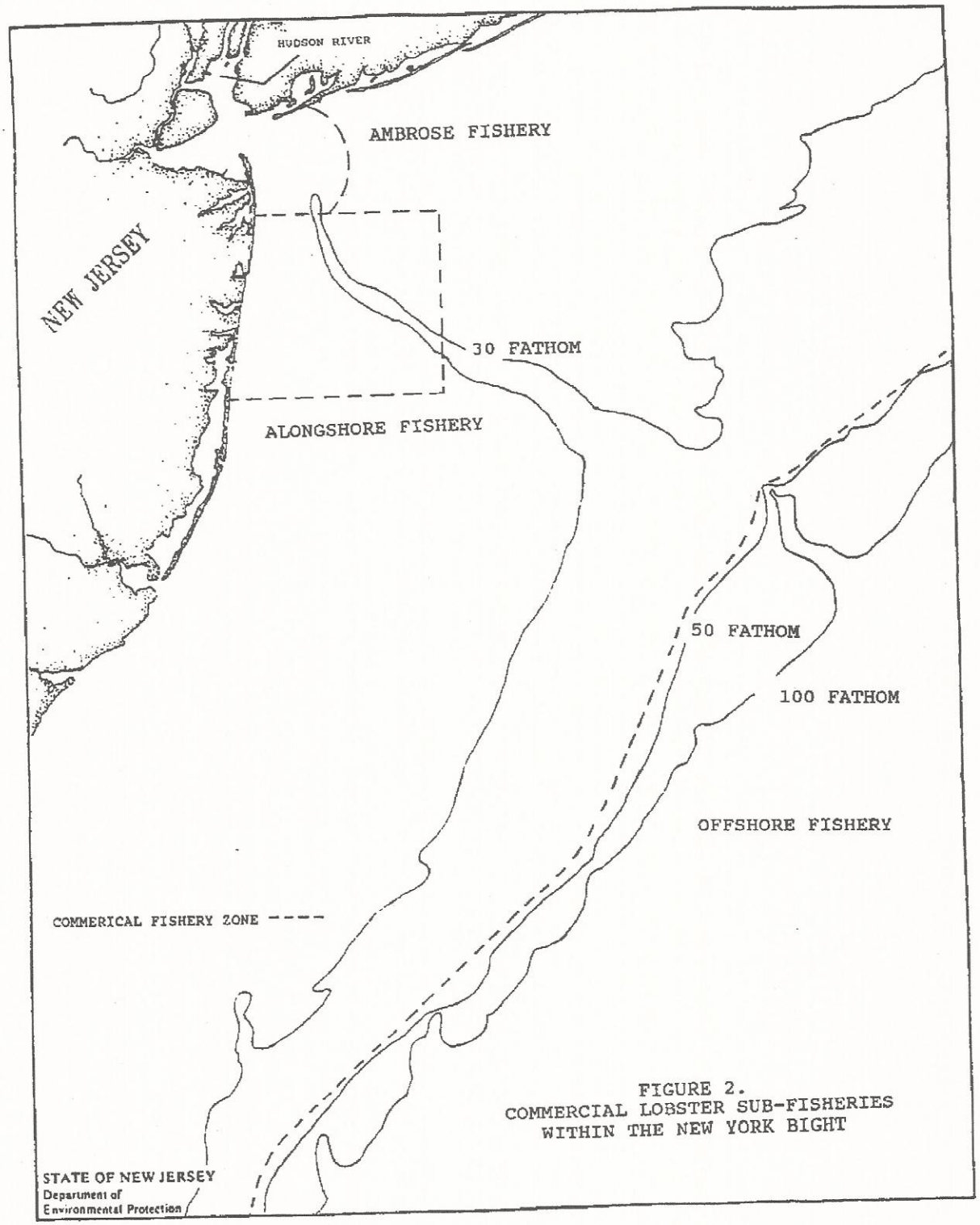

FIGURE 2.
COMMERCIAL LOBSTER SUB-FISHERIES
WITHIN THE NEW YORK BIGHT

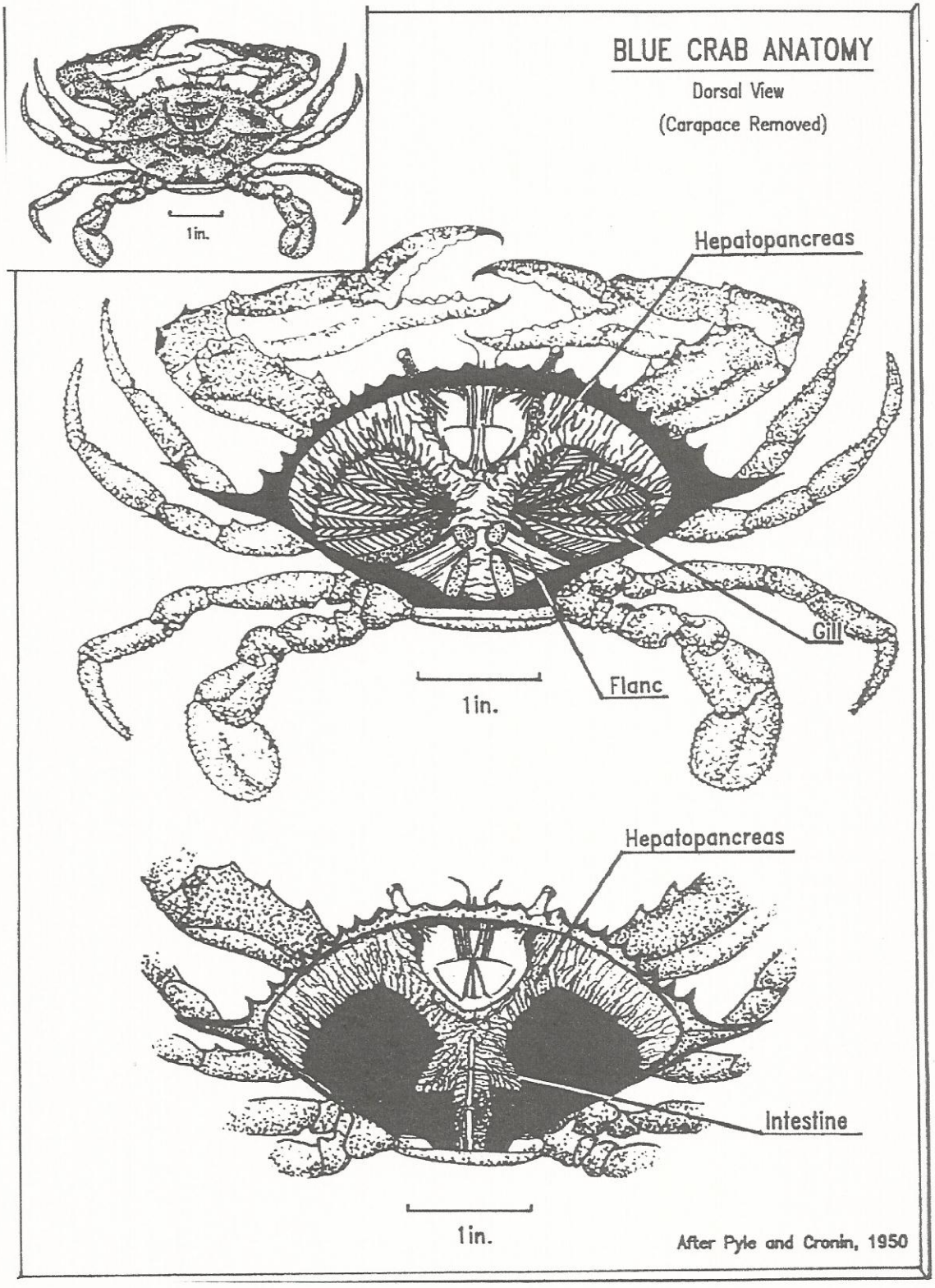

Figure 2a. Blue Crab Anatomy

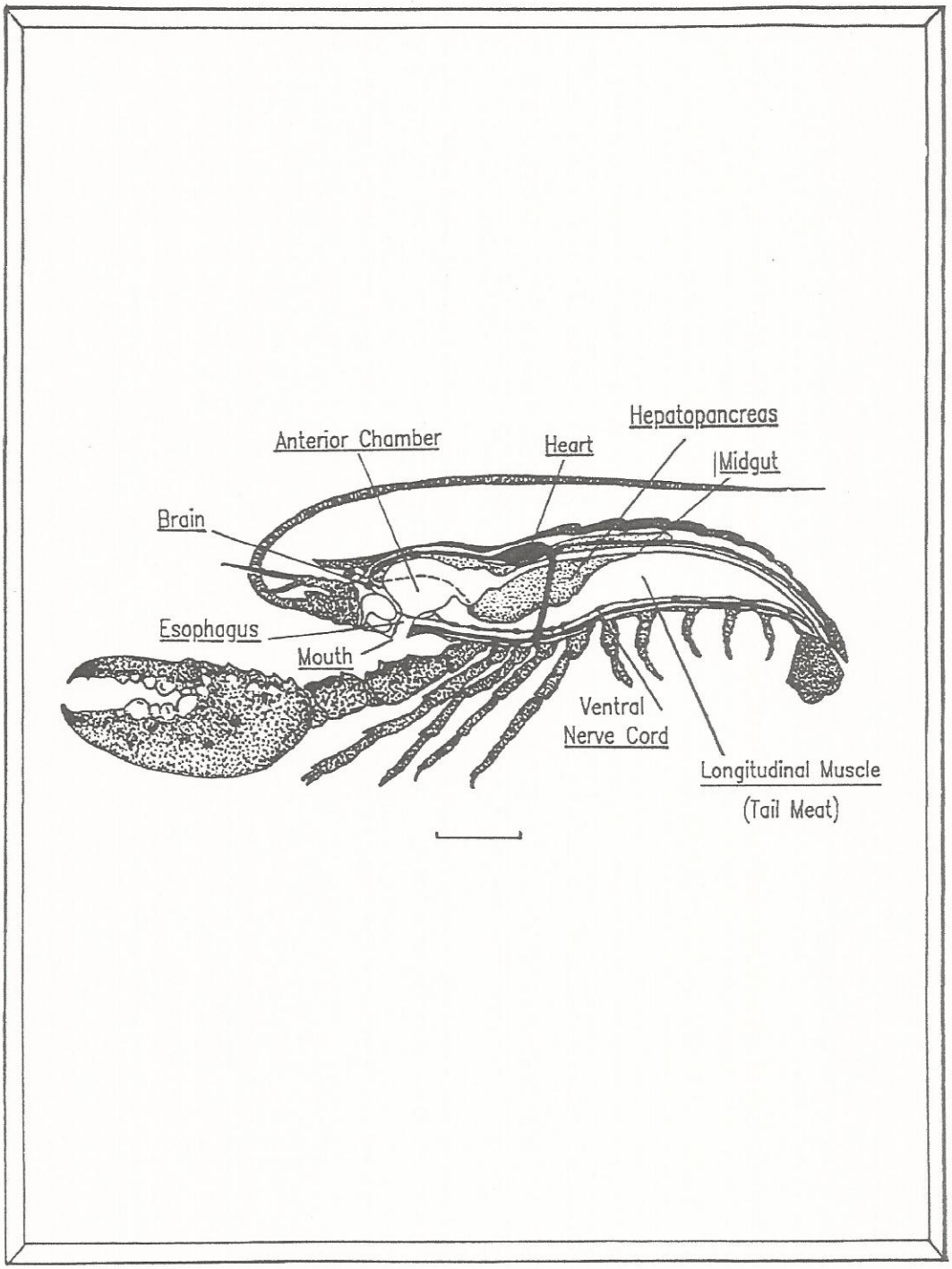

Figure 2b. American Lobster Anatomy

Figure 3. 2,3,7,8-TCDD, 2,3,7,8-TCDF and TCDD Equivalents in Blue Crabs from Raritan Bay and the Lower Hudson River

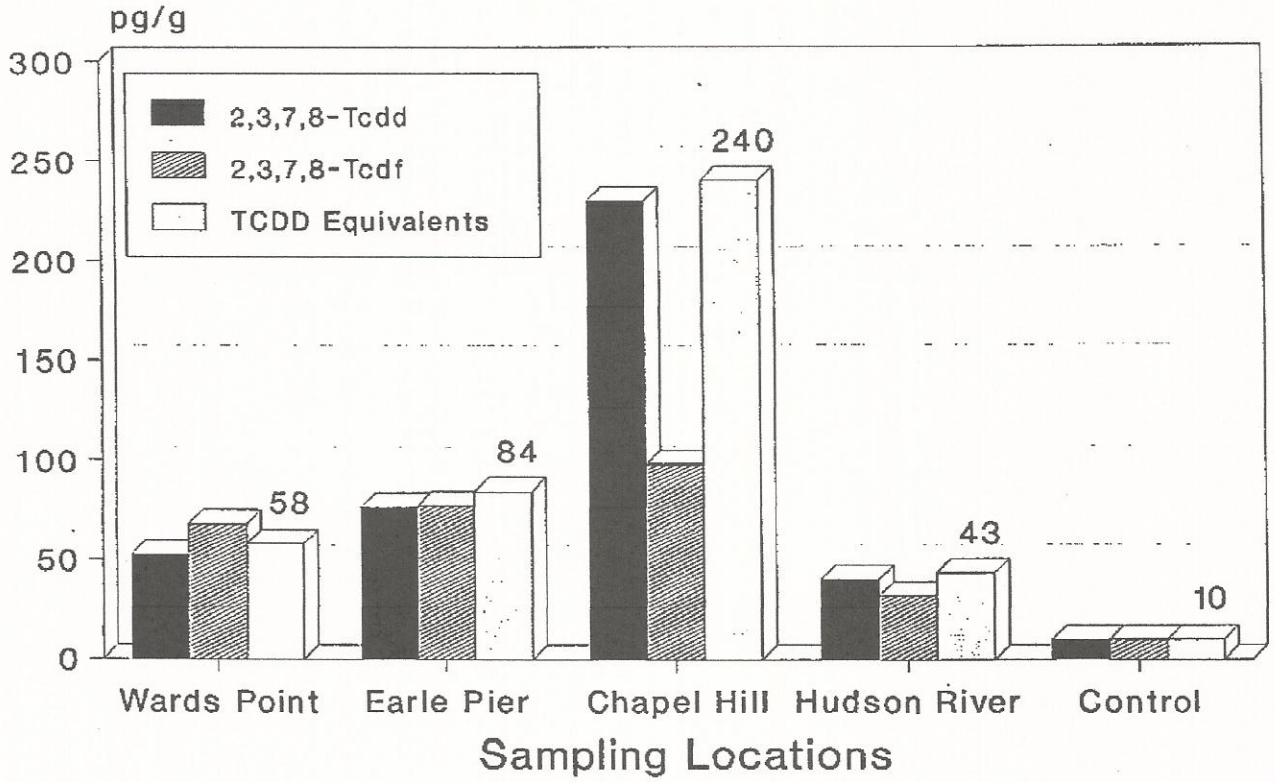

TCDD Equivalents via Barnes et al 1986
Controls are from Delaware Bay,
10 pg/g is the method detection limit.

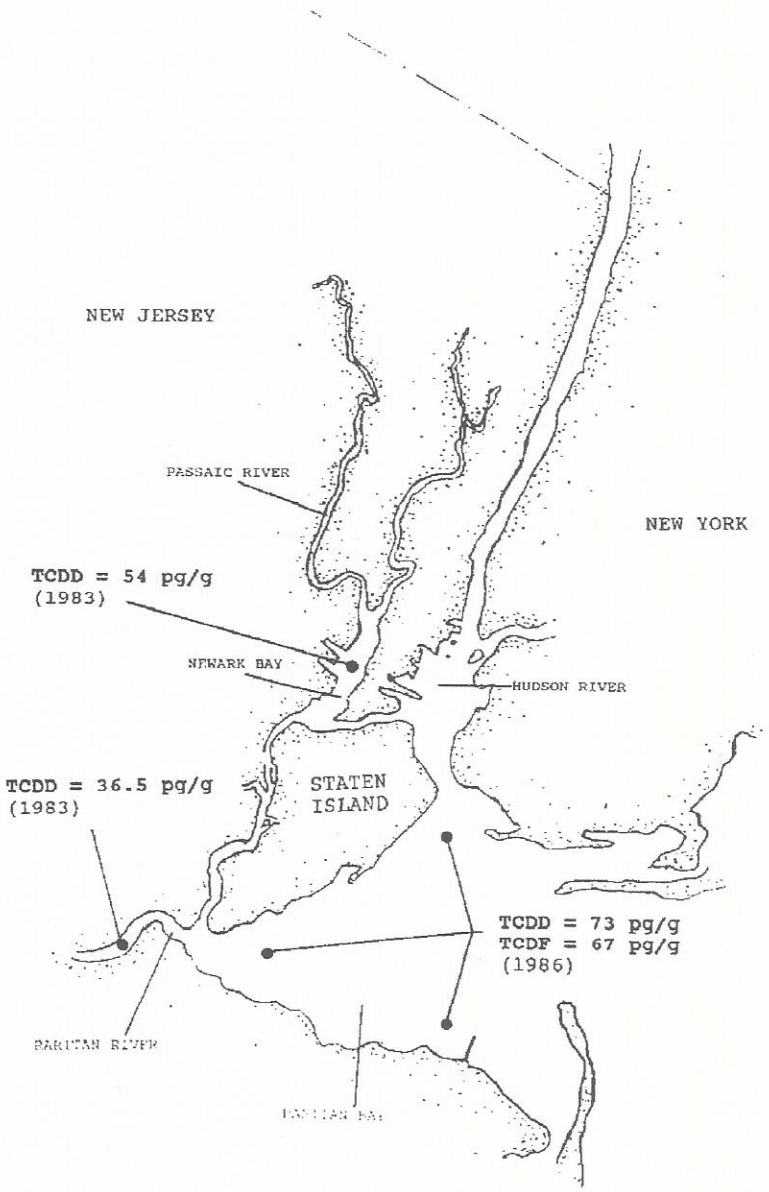

MEAN 2,3,7,8-TCDD/TCDF IN BLUE CRABS
FROM HUDSON-RARITAN ESTUARY
(1983-1986)

Figure 3a.

Figure 4. 2,3,7,8-TCDD, 2,3,7,8-TCDF and TCDD Equivalents in Lobsters from Sub-Fisheries in the New York Bight

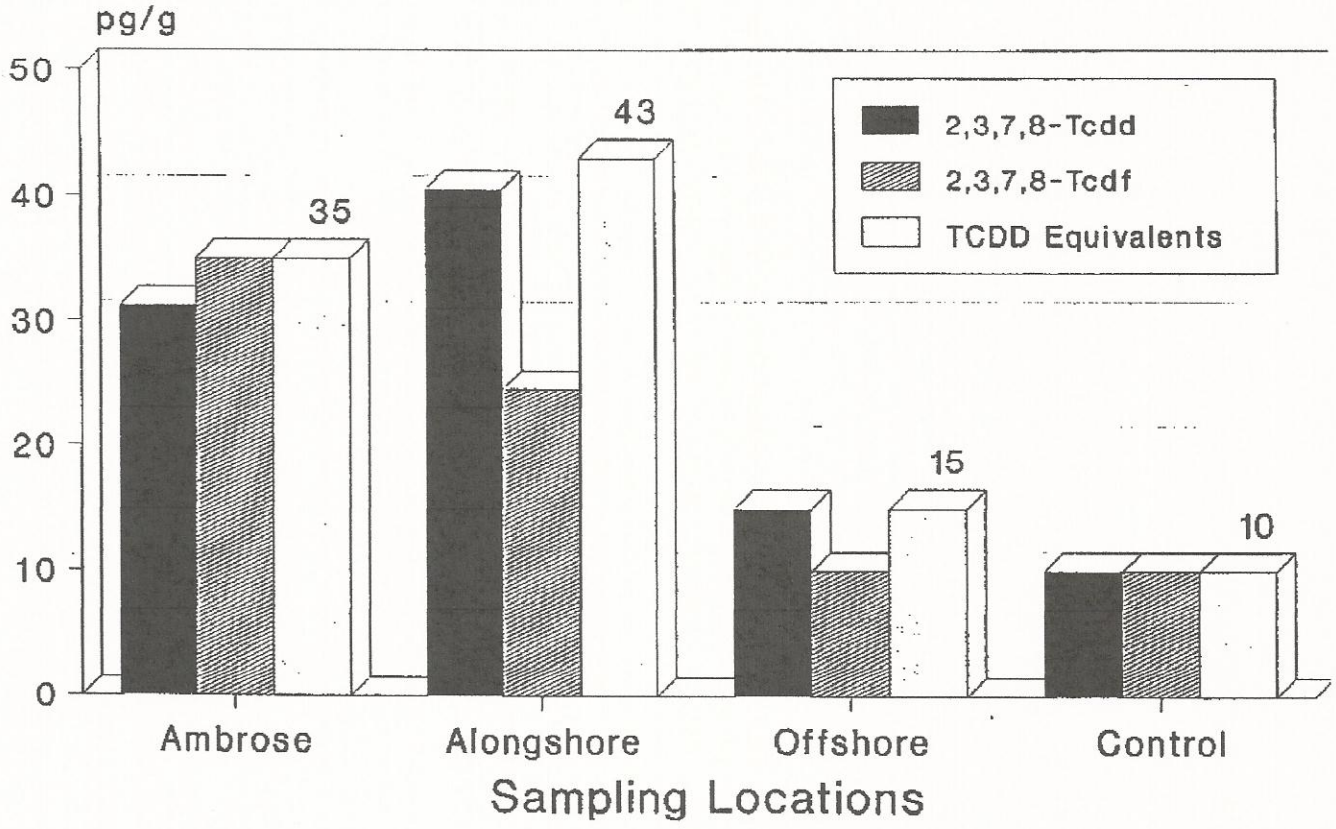

TCDD Equivalents via Barnes et al 1986.
Controls are from Maine.
10 pg/g is the method detection limit.

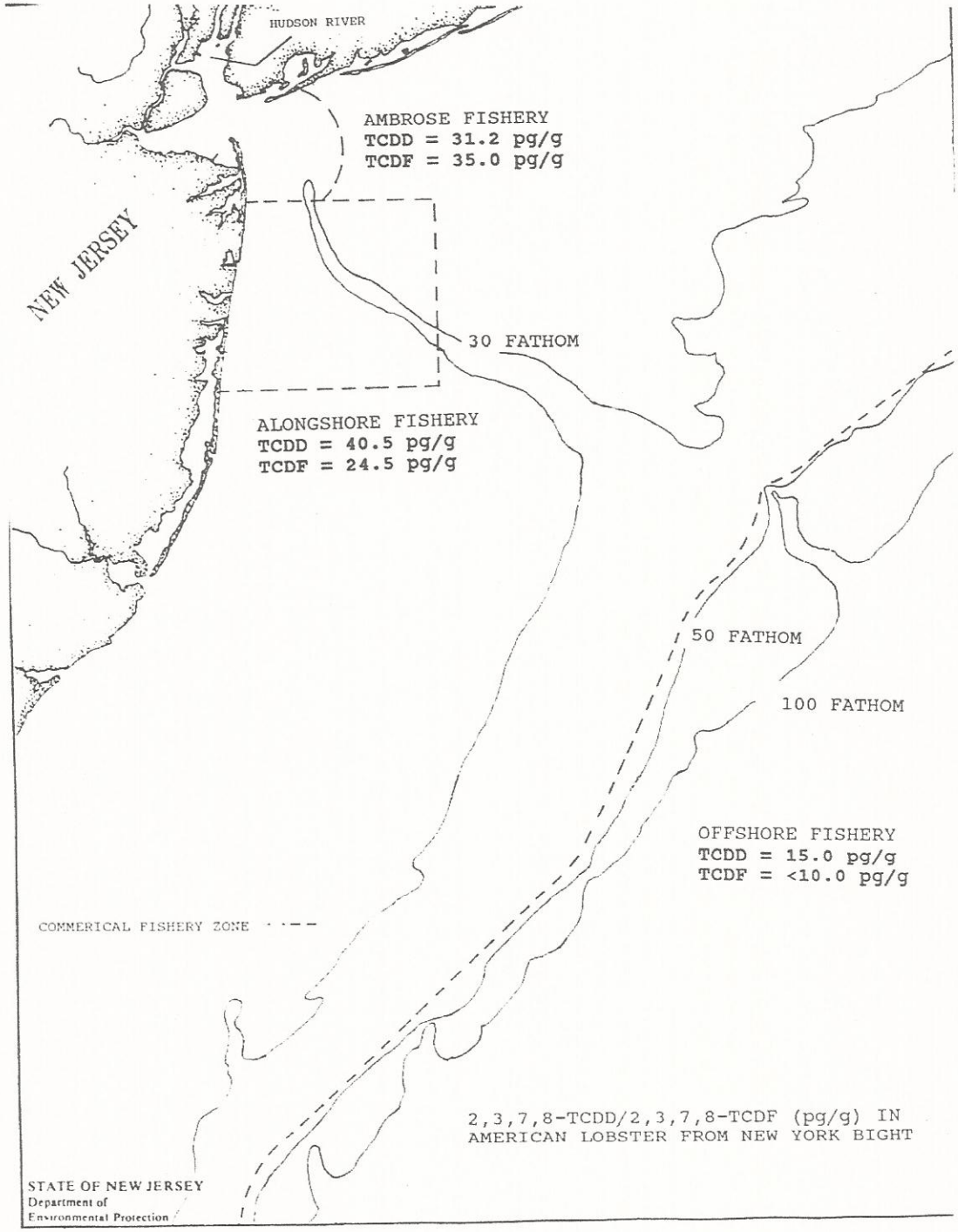
HUDSON RIVER
AMBROSE FISHERY
TCDD = 31.2 pg/g
TCDF = 35.0 pg/g
NEW JERSEY
30 FATHOM
ALONGSHORE FISHERY
TCDD = 40.5 pg/g
TCDF = 24.5 pg/g
50 FATHOM
100 FATHOM
OFFSHORE FISHERY
TCDD = 15.0 pg/g
TCDF = <10.0 pg/g
COMMERICAL FISHERY ZONE
2,3,7,8-TCDD/2,3,7,8-TCDF (pg/g) IN
AMERICAN LOBSTER FROM NEW YORK BIGHT
STATE OF NEW JERSEY
Department of
Environmental Protection

Figure 4a.

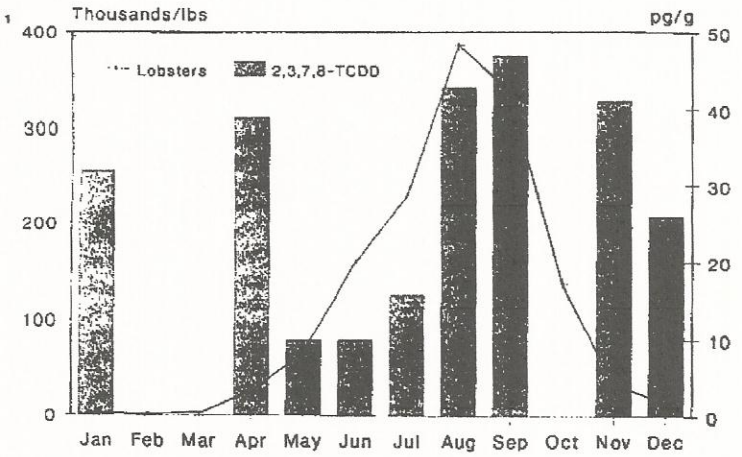

Figure 5a. Landings and 2,3,7,8-TCDD Levels in New York Bight Lobsters

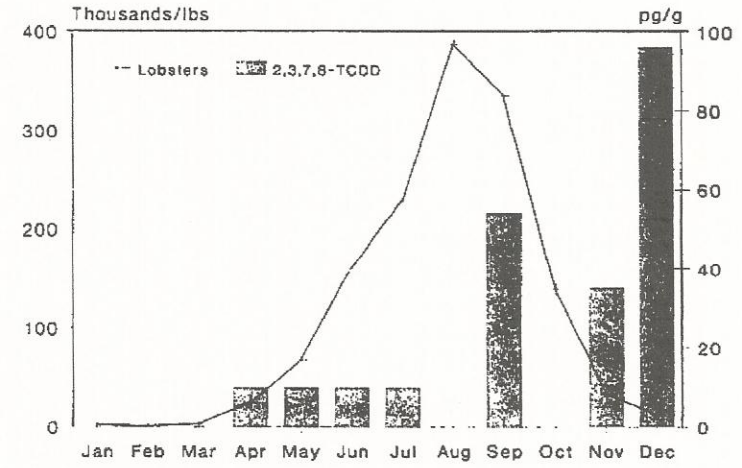

1985-86 Toxics Data; 1987 Landings
10 pg/g is the method detection limit.

Figure 5b. Ambrose Fishery

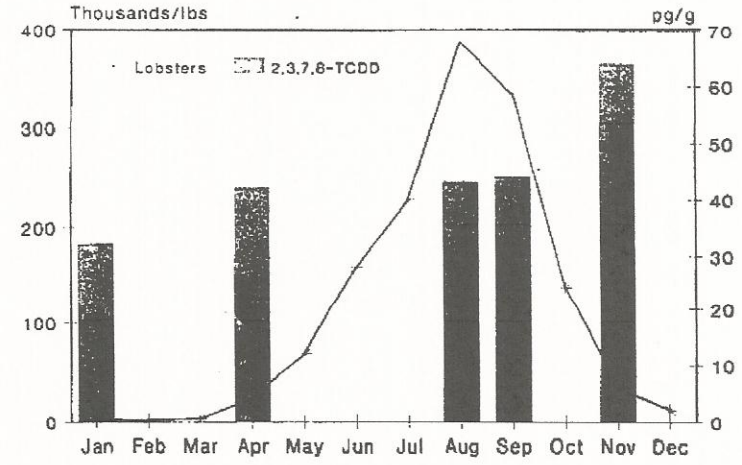

Figure 5c. Alongshore Fishery

FIGURE 5a,b,c.

Figure 6a. Mean 2,3,7,8-TCDD in Lobsters
by Location and Migration Period

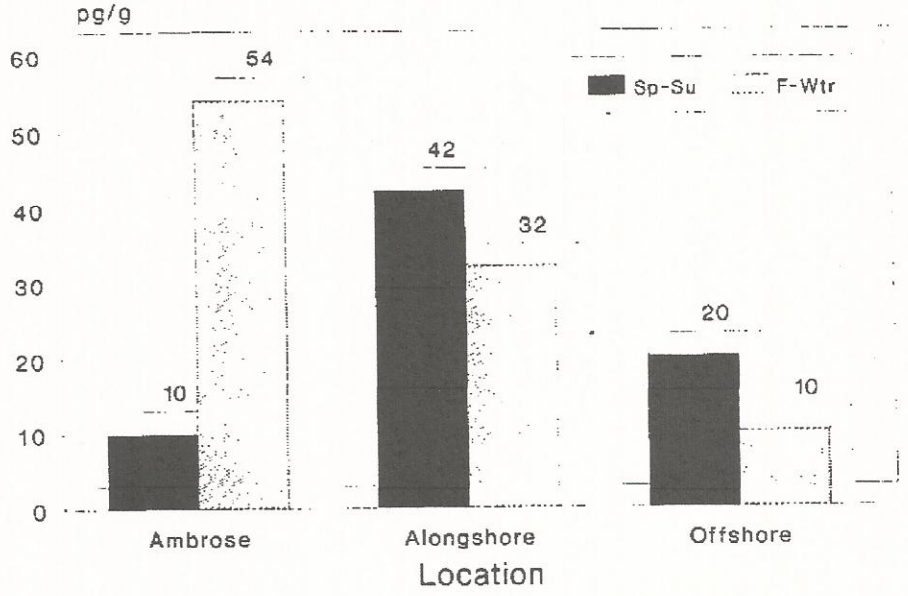

S-Su is Onshore Migration
F-Wtr is Offshore Migration

Figure 6b. Mean 2,3,7,8-TCDF in Lobsters
by Location and Migration Period

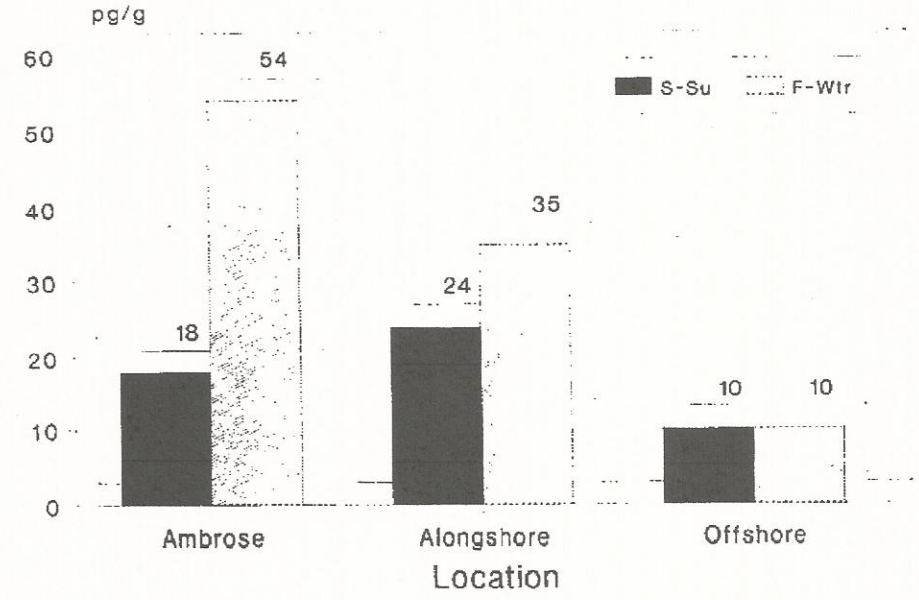

S-Su is Onshore Migration
F-Wtr is Offshore Migration

FIGURE 6a,b

Russian Journal of Marine Biology, Vol. 30, No. 1, 2004, pp. 43–50.

ECOLOGY

Present-Day State of Coral Reefs of Nha Trang Bay (Southern Vietnam) and Possible Reasons for the Disturbance of Habitats of Scleractinian Corals

D. S. Pavlov[1,3,4], A. V. Smurov[2,3], L. V. Il'yash[3], D. N. Matorin[3], N. A. Kluyev[†1], S. V. Kotelevtsev[3], V. S. Rumak[4,1], and T. G. Smurova[2]

[1] *Institute of Ecology and Problems of Evolution, Russian Academy of Sciences, Moscow, 117701 Russia*
[2] *Ecological Center, Moscow State University, Moscow, 119992 Russia*
[3] *Biological Department, Moscow State University, Moscow, 119992 Russia*
[4] *Russian–Vietnamese Tropical Center, Hanoi, Vietnam*
e-mail: info@ecocenter.msu.ru

Received October 10, 2003

Abstract—Our investigations were conducted from 1990 to 2002. Sampling of bottom sediments and biological objects, as well as photo and video shooting, were performed during scuba diving. The state of the environment and coral reef communities was assessed using the chemical–analytical, fluorometric, and luminometric methods, as well as the Ames test and the transect technique. The research results suggest that the spectrum and distribution pattern of persistent congeners of PCDD/Fs (dioxins) in bottom sediments are similar to those of the defoliant "Agent Orange" and that the bottom sediments are toxic and display photo inhibition and a mutagenic effect. The bottom of the bay is heavily silted throughout its depth. Many large dead colonies of corals without mechanical damage were observed everywhere. The total coverage by live corals in all sites investigated does not exceed 30%. Although, without a doubt, many factors contributed much to the disturbance of the bay ecosystems, the actual trigger for the degradation of the coral reefs seems to be the input of dioxin-containing chemicals used as defoliants during the American–Vietnamese war (Vietnam War).

Key words: Coral reefs, scleractinians, ecodiagnosis, ecotoxicology, dioxins, defoliants, "Agent Orange."

In recent decades, there has been a tendency toward the deterioration of the state of near-shore coral reefs in various regions of the world [15, 22, 24–26], and for Vietnam in particular, it has become a challenge. Vietnam has extensive sea borders, and the biological resources of the sea are of great importance in the economy of the country. The productivity of the coastal waters is largely determined by the state of the corals reefs.

It has been reported that Nha Trang Bay (South China Sea) has favorable biotopes and one of the richest scleractinian faunas in Vietnam [4, 5, 19, 23]. A series of monographs "Scleractinian Corals of Vietnam" provided a detailed account of the species composition and distribution of scleractinians in Nha Trang Bay up to the year 1986 [6–9]. The purpose of the present research is to examine the present-day state of near-shore coral reefs in Nha Trang Bay and to make a comprehensive integral evaluation (ecological diagnostic) of the quality of the benthic environments and to clarify the possible reasons for the degradation of the coral reefs of the bay.

MATERIALS AND METHODS

In planning this research and in our analysis of the results, we used, along with other publications and our own data, the available reports of expeditions of the Institute of Marine Biology (IMB, then of the Far Eastern Branch of the USSR Academy of Sciences) for the years 1981, 1982, and 1986, as well as the reports of the Russian–Vietnamese Tropical Center (Russian Academy of Sciences) and the Institute of Oceanography (National Center for Scientific Research of Vietnam) in Nha Trang.

The investigations were carried out from 1990 to 2002 at 60 stations, which were located practically throughout the bay (Fig. 1).

In planning the research, we singled out four transects within the bay:

1. Transect A—the northern bay. In this part of the bay, there is a large coral bank (stations 41, 42, 43, 44), the islands of Dum (station 45) and Tyala (station 49), and Binhkanh Bay (stations 46 and 47) with numerous shrimp farms and the Ngada River emptying into the bay.

2. Transect B—the entrance channel of the Kay River. Here, between the coral bank and Che Island

1063-0740/04/3001-0043 © 2004 MAIK "Nauka/Interperiodica"

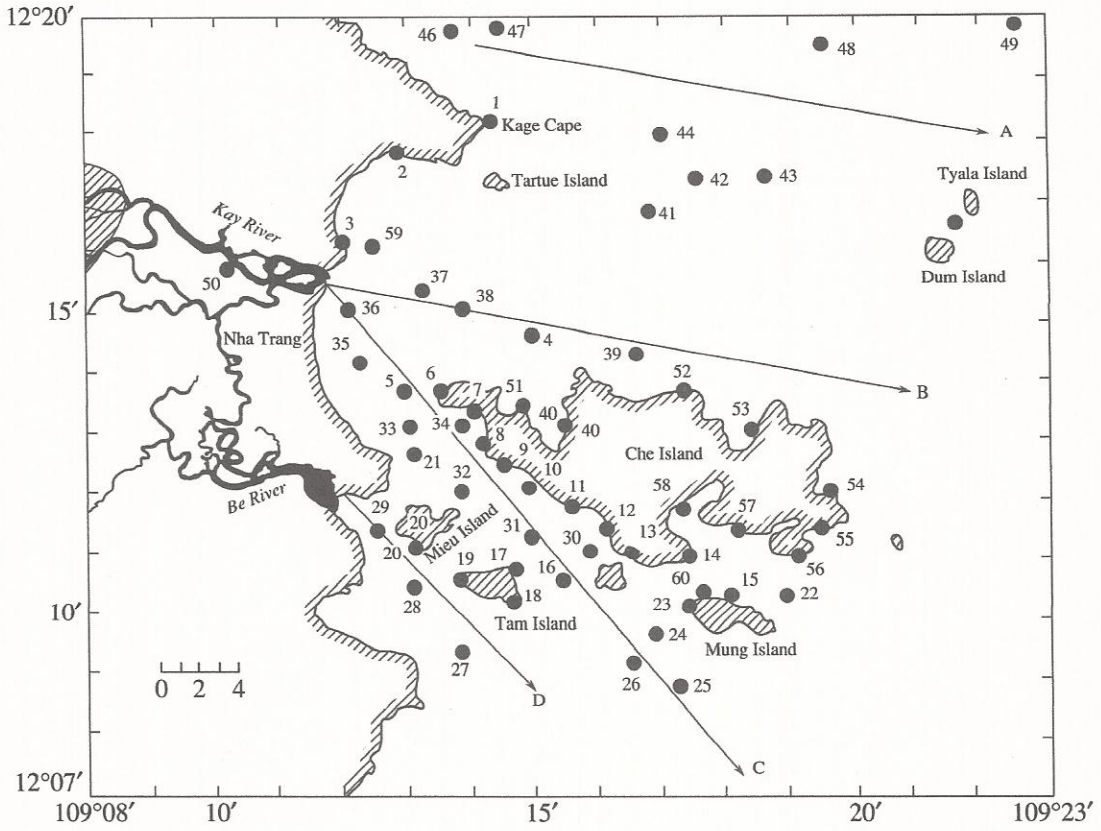

Fig. 1. The location of stations in Nha Trang Bay, 1990–2002. The shaded patch in the upper reaches of the Kay River (left upper part of the map) is the lower limit of the area where dioxin-containing defoliants were used during the American–Vietnamese war (Vietnam War). Transects A, B, C, and D are shown by arrows (explanation in the text).

(stations 4, 37, 38, 39) at a depth of 15–20 m, a non-silted sand plateau was observed in the late 1980s and the early 1990s.

3. Transect C—the area between Che Island and the islands of Mieu and Tam. By virtue of the hydrological features of the bay, a large part of the suspended material from the Kay River is deposited here.

4. Transect D—the southern bay. It receives suspended material from the Be River.

Analyses were performed in the Laboratory of Ecotoxicology, the Institute of Ecology and Evolution Problems, Russian Academy of Sciences. In the bottom sediment samples collected at stations 5, 16, 20, 21, 24, 27, 29, 30, 33, 36, 37, 39, 41, 44, 49, and 50, the total content of dibenzo-p-dioxins (PCDD) and dibenzofurans (PCDF) (in all, 17 congeners) was determined by high resolution chromato-mass spectrometry and expressed using the international equivalents of toxicity (1-TEQ or dioxin equivalent) relative to the most toxic congener 2,3,7,8-TCDD [3]. Specific isomer analysis of PCDD and PCDF was carried out on a GC-MS "Finnigan" MAT-95XL, Hewlett Packard HP 6890 Plus, at a resolution of 10000 [20]. Dioxins are long-lived superecotoxicants [3, 18] and mask well less persistent compounds (among them toxic), the components of which they were formerly.

As is customary in chemico-analytical research, for averaging of small-scale nonuniformity in the distribution of the constituents of bottom sediments, samples at each station were taken at 4–5 points lying about 1 m from each other. Bottom sediments were removed to a depth of 10–15 cm (on hard sands) or 50–70 cm (on soft silts). Samples collected at the same station were pooled, while under water, into an integrated sample and placed in a 1.5-liter tightly sealed plastic vessel. Subsamples of the integrated samples were used in the toxicological research.

The following biological methods of environmental diagnostic [14] were used: fluorimetric, bioluminometric, and genetic methods and the transect technique.

Coral coverage and the state of bottom communities were assessed using the transect technique. Scleractinian corals were selected as the major object of study because, as was noted above, they are edificatory species indicative of the state of coral communities. Transects were made at stations 1, 3, 6, 11, 12, 15, 18, 19, 23, 25, 40, 42, 46, 47, and 49. The transect (graduated rope 100 m long) was perpendicular to the shore-

line starting with a zero depth. Along the transect, at 10 m intervals, photo and video shooting of objects was made within a 1 × 2 m aluminium frame with internal 25 × 25 cm quadrates.

Sediment sampling and photo and video shooting were made during scuba diving. The exact position of station was fixed from the ship using a Garmin GPSIII plus; where possible, the location of stations was tied to on-land reference points. The depth and transparency of the water were registered at each point of sampling.

The toxicity of the bottom sediments in the bay was studied using samples collected on four transects at stations 5, 16, 20, 24, 27–29, 30, 32, 33, 36, 37, 39, 41, 44, 47, 49, and 59, which more or less fully represent the diversity of the biotopic and hydrological characteristics of the bay. In addition, a sample of sediments from the former riverbed of the Kay River, which is completely inundated during the floods (station 50), was analyzed.

The effect of bottom sediments on photosynthetic activity was examined using cultures of the marine algae *Thalassiosira weissflogii* (Grunow) Fryxell et Hasle (Bacillariophyta), *Tetraselmis viridis* (Rouch) Morris (Prasinophyta), *Nannochloris* sp. (Chlorophyta), and *Isochrysis galbana* Parke (Prymnesiophyta). These algae—routine objects of marine toxicology—belong to the main large taxonomic groups of native inhabitants of marine plankton and periphyton. Scleractinian corals harbor photosynthgetic organisms (zooxanthellae), and fluorimetric studies were made to reveal the adverse effects of the environment on the zooxanthellae, which inevitably tell on the coral host [16]. The working concentration of the bottom sediment suspension in toxicological experiments was 20 mg/ml. Cultures (10 ml) without bottom sediment suspension were the control. Photosynthetic activity (PA) was estimated by the relative proportion of pulse-amplitude-modulation fluorescence $q = F_v/F_m = (F_m - F_o)/F_m$ when measuring the chlorophyll fluorescence rate in open (F_o) and closed (F_m) reaction centers [10]. F_o and F_m in algal suspension were recorded with a portable two-beam impulse fluorimeter designed by the Chair of Biophysics of the Biological Faculty of Moscow State University [1]. The impulse duration of the testing excitation light of fluorescence was 4 μs; the average power density of the exciting light in the measurement of F_o and F_m was 0.4 and 3000 Wt/m^2, respectively. The fluorescence rate was measured before adding the bottom sediment suspension and 24, 48, and 72 h after the addition; the same was done to the control cultures at the same time intervals. Prior to measurements, the algal cultures with the bottom sediment suspensions added were thoroughly stirred. A series of methodical experiments showed that at a sediment concentration of 20 mg/ml, the suspension of particles does not interfere with the estimation of the fluorescence parameters of the algae. From the q values, the inhibition coefficient of PA was estimated:

$$K_{PA} = (1 - (q_{exp}/q_{contr})) \times 100\%,$$

where q_{exp} is the relative contribution of pulse-amplitude-modulation fluorescence in algae in the experimental cultures exposed to the bottom sediment suspension; and q_{contr}, in control cultures. The methodical tests showed that the standard deviation value of K_{PA} changes in some cultures in the range from 0 to 9%; hence, K_{PA} values exceeding 2δ (18%) were considered significant.

The effects of bottom sediments on the vital activity of aerobic nonphotosynthesizing heterotrophic bacteria, as well as the degree of integral toxicity of the bottom sediments were evaluated using the "Biotox-6" and "Biotox-10" devices. This investigation was undertaken because heterotrophic bacteria are important in maintaining the near-shore ecosystem stability in the South China Sea [15] and because an integral evaluation of the toxicity of the bottom sediments for humans is needed. The rate and degree of suppression of the bioluminescence of biosensors was measured. The biosensors were test cultures of heterotrophic chemoluminescent bacteria. The response of the bacteria to supplemented substances is analogous to that in other living organisms, and the value of 50% fluorescence quenching in bacteria completely correlates with a 50% lethal dose for humans. The intensity of bioluminescence of special biosensors ("Ecolum" biosensor in our investigations) containing chemoluminescent bacteria changes in relation to the toxic effect and is represented by the index of toxicity [2, 11]

$$T = 100(I_o - I)/I_o,$$

where I_o and I are respectively the intensity of fluorescence of the control and the experiment at a fixed time of exposure of the test solution with the test object. According to the "Biotox" user's manual [12], a value of the toxicity index from 0 to 20 indicates that the test substances are virtually nontoxic; with index values of 20 to 50, the test substance is toxic; and with values exceeding 50, toxicity is high. Negative values of the toxicity index are indicative of the presence in samples of substances stimulating metabolic processes in bacteria. In tests with chemoluminescent bacteria, the procedure for the preparation of bottom sediment suspensions was analogous to that used in the fluorimetric study. Samples of bottom sediments were dried and ground in porcelain dishes, then 5 g of the sediment was diluted in 25 ml of filtered pasteurized seawater (distilled water for river samples) to attain a working concentration of 20 mg/ml. For each sample, the toxicity of the suspensions was measured in 12 replicas.

Increased mutagenicity of the environment is one of the factors that not only induces negative responses in some organisms (including humans), but also disturbs the stability of the population structure and ecosystems as a whole. Mutagenic effects of bottom sediments were evaluated using generally accepted methods. Acetone–hexane extracts were made from dried (to con-

Table 1. Mutagenic index of extracts from the bottom sediments in the presence of (+MA) and without (–MA) the metabolic activation system of the strain TA-98 sensitive to mutagens inducing the shift of the reading frame of the genetic code and the strain TA-100 sensitive to mutagens causing mutations of the base substitution type

Reagent			Dose per petri dish	*Salmonella typhimurim* strains			
				TA-98		TA-100	
				+MA	–MA	+MA	–MA
Control	DMSO		0.1 ml	1.0	1.0	1.0	1.0
	2- aminoanthracene		0.5 g	**44.8**	0.9	**8.5**	1.0
Extracts of bottom sediments from stations	River	50	0.1 ml	1.1	**2.3**	0.9	1.5
	Transect C	36	0.1 ml	0.9	0.9	**2.6**	**2.0**
		5	0.1 ml	**1.8**	1.6	0.7	0.9
		30	0.1 ml	**5.4**	1.6	1.0	1.3
	Transect D	29	0.1 ml	**3.0**	1.1	0.9	1.2
	Transect A	44	0.1 ml	**1.8**	**1.9**	0.8	1.2

Note: Bold-faced numerals indicate a significant mutagenic effect.

stant mass at 50°C) bottom sediment samples. The extracts were evaporated, dissolved in dimethylsulfoxide (DMSO), and tested according the Ames method in three replicas. A positive control test with promutagen 2-aminoanthracene was run simultaneously. *Salmonella typhimurim* TA-98 and TA-100 strains were used. The strain TA- 98 is sensitive to mutagens inducing the shift of the reading frame of the genetic code, while TA-100 is susceptible to mutagens causing mutations of the base substitution type. Promutagens (mutagens present in the environment in the inactive state) were revealed according to the standard method [21] using the metabolic activation of bottom sediment extracts. The results of tests (Table 1) are represented as the mutagenic index (MI) reflecting the ratio of the number of colonies his^+ *Salmonella* revertants in the experiment to the control (DMSO). With MI from 1.7 to 10, the mutagenic effect was considered positive; from 10 to 100, moderate; and more than 100, high [17].

RESULTS

Long-term studies of the bottom biotopes using the transect method revealed a more or less pronounced tendency toward the degradation of coral reefs, siltation, and the suppression of scleractinians at all depths and at all stations in the bay. We compared the results of charting coral reefs made by T.A. Britaev and M.V. Pereladov (unpublished report of the Tropical Center for 1990) and the results from our survey in the early 1990s at stations 8, 9, 11, 12, 13, 14, 51, 40, and others adjacent to Che Island with the data obtained by the expeditions of the IMB in 1983 and 1986. Over the following 6–7 years, once rich scleractinian settlements had degraded markedly but still remained. By 2001, in many areas neighboring Che Island scleractinian settlements had disappeared almost completely; dead corals overgrown with periphyton, coral debris covered with silt, or even continuous silt fields were observed on the bottom. Particularly marked siltation occurred in the western and southern bay in the area between Che Island and the mainland (transects C and D, stations 5, 16, 21, 25–33, 35–37, and 59; see Fig. 1). In extensive areas of the bay, the silt thickness was up to several tens of centimeters. In bottom areas where the silt layer exceeded 1–3 cm, live scleractitians were completely lacking. Young scleractinian colonies (seldom more than 10 cm in diameter) or small end growths on old dead colonies of branched corals occurred in weakly silted areas of the bottom (Fig. 2b). Relatively large colonies (up to several tens of centimeters in diameter) were usually encountered on boulders, raised fragments of dead coral reefs, or elevations of the bottom (Fig. 2a).

Earlier ([4, 6], unpublished reports of expeditions of the IMB and the Tropical Center of the RAS until the year 1990), Nha Trang Bay was characterized by a high coverage (up to 100%) of the substratum with live corals in coral habitats. Toward the end of the study period, large dead coral colonies without mechanical damage were found everywhere (Fig. 2c). Mainly small (young) specimens of other hermatypic coral species were found. The total live coral coverage was not above 30% at all points surveyed. The maximum coverage was found for the near-shore reefs of Cape Kage (Station 1), Mung Island (stations 15 and 60), and Tam Island (station 19), where at depths down to 10 m a considerable quantity of live corals was observed on the bottom elevations (ridges) against the background of the silty bottom between the ridges (Fig. 2a).

The fluorimetric studies showed that in most cases the photosynthetic activity was inhibited after a 1-day exposure of algae with bottom sediment suspension and sensitivity varied among the algal species (Table 2). Pooling the data on the suppression of photosynthetic

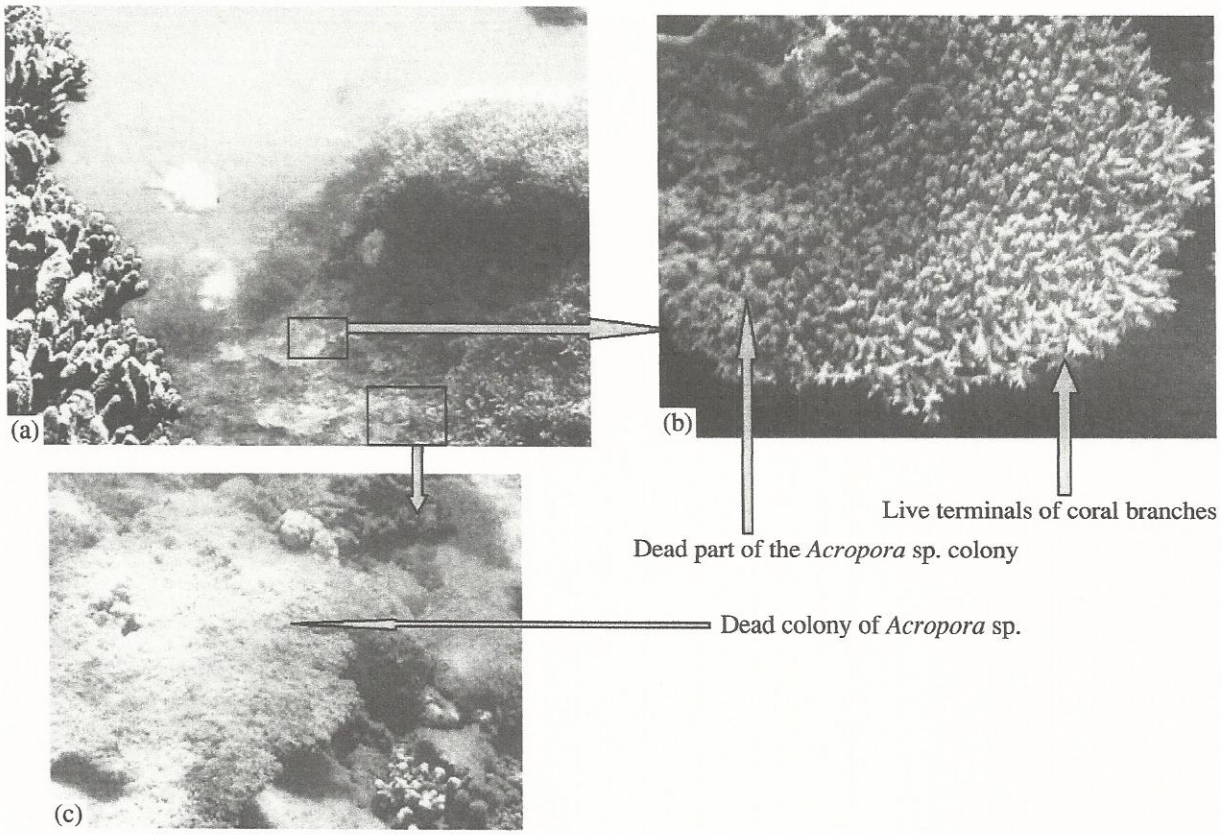

Fig. 2. Station 15 (Mung Island). Depth is about 4 m and transparency about 12 m (see text for explanation).

activity 24 h after supplementing the bottom sediment suspension for four test cultures, we calculated the average values of $^{24}K_{PA(avg)}$ (Table 2), which, to some degree, represent the total response of the multispecies natural community of photoproducers. Most of the tested samples exerted a significant inhibitory effect on photosynthetic activity (Table 2). Inhibition of photosynthetic function was highest ($^{24}K_{PA(avg)}$ = 60%) with the bottom sediments sampled at station 5. In most cases (10 stations), the values of $^{24}K_{PA(avg)}$ varied in the range of 23–37%. In *Nannochloris* sp. exposed to the bottom sediment suspension with the highest content of dioxins (4–20 ng/kg) (stations 16, 33, and 59), K_{PA} increased on the 2nd–3rd day, while at a dioxin concentration of less than 4 ng/kg, K_{PA} decreased with time (Table 2). The exception was a decrease in K_{PA} after the first day of exposure with sediments from the former bed of the Kay River at a dioxin concentration of 7.9 ng/kg (station 50). It is possible that the decrease was due to the different composition of toxic substances in the sediments of the river and the sea bay.

The data on the effect of bottom sediment suspension on bioluminescence agreed well with the data on photosynthetic activity (Table 2). A pronounced toxic effect on bacteria was found for sediments from almost all of Nha Trang Bay, excluding stations 20, 27, 28, 29 (channel of the Be River), station 49 at Tyala Island (which is the farthest from the mouth of the Kay River), and station 47 in Binhkanh Bay. Despite the strong anthropogenic impact (except station 49), bottom sediments from these points produced a pronounced positive effect, increasing bioluminescence. Bottom sediments from the cutoff meander of the Kay River (station 50), despite the high dioxin content (I-TEQ = 7.9), induced no pronounced inhibition of bioluminescence. Bioluminometric data, along with the results of other tests, suggest the toxicity of bottom sediments from transects C, B, and partly A, as well as the mosaic distribution pattern and different present-day composition of toxicants in bottom sediments of the bay.

All the extracts of bottom sediments tested displayed a weak mutagenic effect (Table 1). The extracts of sea bottom sediments showed a mutagenic effect only following metabolic activation and induced a shift of the reading frame of the genetic code. On the other hand, extracts of the bottom sediments from station 36 located in the immediate proximity of the Kay River mouth and sediments from station 44 (coral bank) showed a direct mutagenic effect, which was retained after metabolic activation. Bottom sediment extracts from station 36, in contrast to all others, caused mutations of the base substitution type. River sediment

Table 2. Inhibition of the photosynthetic activity of algae (% of the control) on 24, 48, and 72 h exposure and of chemoluminescence of heterotrophic bacteria (toxicity index) in the presence of the bottom sediment suspension

Transect	Station	Depth, m	1-TEQ, ng/kg	Coefficient of inhibition of algae photosynthesis (K_{PA}) on 24, 48, and 72 h exposure												$^{24}K_{PA}$ (avg)	Toxicity index (I_t) for 30 min exposure
				Tetraselmis viridis			*Nannochloris* sp.			*Isochrysis galbana*			*Thalassiosira weissflogii*				
				24	48	72	24	48	72	24	48	72	24	48	72		
River	50	1.5	**7.9**	37	21	15	22	16	14	41	42	29	38	30	20	**35**	15
C	36	15.4	**2.4**	28	30	20	14	17	14	71	87	80	24	27	16	**34**	**44**
	5	25.7	**3.1**	39	38	30	32	32	22	94	69	91	76	41	55	**60**	**49**
	33	22.7	**4.2**	20	24	18	14	12	19	32	15	2	33	25	0	**25**	**73**
	32	19.4	–	8	25	18	11	17	13	24	0	0	18	0	0	15	**44**
	30	21.5	**1.8**	27	20	8	14	19	23	29	8	0	22	0	9	**23**	**62**
	16	20.6	**20.8**	11	17	17	9	17	16	23	0	0	18	0	0	15	**37**
	24	32.7	**0.4**	29	19	23	13	7	5	26	18	10	30	28	14	**25**	**94**
B	59	7.5	**16.8**	27	25	8	20	18	31	30	17	0	31	6	3	**27**	**80**
	37	21.8	**1.9**	14	10	0	9	9	13	22	7	14	8	0	0	13	**70**
	39	20.5	**0.8**	9	4	8	0	3	0	0	18	0	2	0	0	3	**30**
D	29	14.0	**1.0**	21	16	3	8	12	1	16	16	2	26	20	2	**18**	–97
	28	10.6	–	39	29	2	28	19	1	22	21	20	26	26	22	**29**	–47
	27	9.5	**2.1**	58	45	23	24	19	3	22	14	0	42	24	13	**37**	–108
	20	4.5	**0.7**	2	0	0	4	9	0	0	0	0	2	0	0	2	–157
A	41	21.0	**0.8**	29	25	13	15	9	4	31	18	17	15	13	10	**23**	**50**
	44	18.0	**0.5**	2	0	2	0	0	0	0	2	6	0	0	0	1	**49**
	49	18.0	**1.3**	0	0	0	0	0	0	0	8	6	0	0	0	0	–201
	47	5.0	–	–	–	–	–	–	–	–	–	–	–	–	–	–	–65

Note: The depth and total amount of dibenzo-p-dioxins (PCDD) and dibenzofurans (PCDF) represented by the international equivalents of toxicity (I-TEQ) are given for stations of bottom sediment sampling. Bold-faced values indicate a significant toxic effect; "–"—measurements were not made.

extract also induced a direct mutagenic effect, which, however, was lost following metabolic activation. We note that a reduction in the mutagenic index in some experiments, compared to the control (MI < 1), might indicate the presence of compounds toxic to *Salmonella*. Thus, the Ames test, suggesting the presence in bottom sediment samples of mutagens and toxicants, indirectly supports the above assumption on the different present-day composition of toxicants in the bottom sediments of the river and the sea bay.

The results of chromatographic and mass spectrometric analyses revealed the presence of persistent congeners PCDD and PCDF in bottom sediment samples from the bay. The spectrum and distribution pattern of congeners in all samples were close to those of the defoliant "Agent Orange" (predominantly 2,3,7,8-TCDD, 1,2,3,4,6,7,8-HpCCD, OCCD, and 1,2,3,7,8,9-HxCDF, OCDF). The total amounts of dioxins in the bottom sediments at sampling stations varied from 0.409 to 20.806 ng/kg in I-TEQ (Table 2), which is several orders of magnitude higher than the accepted sanitary standards.

DISCUSSION

The impairment of the state of near-shore coral reefs in Nha Trang Bay has been explained by various reasons. Among them global warming of the climate, much increased recreation pressure and coral harvest for souvenirs, injurious use of corals for lime production, fishing with the use of explosives, and pollution of the Kay and Be rivers by agricultural and municipal waste water.

Our integral assessment of the state of the bottom habitats in the bay suggests that bottom sediments contain long-lived components of herbicide chemicals of the "Agent Orange" type and that the environment is unfavorable (toxic) to many groups of organisms in the greater part of the bay. The diagnostic data allow us to come back to the earlier hypothesis [13] that despite the undeniable and apparently considerable adverse affects of the above factors on the bay's ecosystems, one of the most probable reasons and a trigger for the degradation of the reef-forming communities were toxic dioxin-containing components of herbicides, which were used as defoliants during the American–Vietnamese war (Vietnam War) and have entered the bay via the Kay River run-off.

In the basin of the Kay River and its tributaries, hundreds of thousands of highly toxic defoliants were sprayed in the course of military operations. Both soluble and little-soluble highly toxic components of dioxin-containing chemicals were transferred into the bay via floodwaters and heavy fractions of river silts and detritus. The range of long-lived ecotoxicants (PCDD and PCDF) in the modern sediments of the river and the bay bears a sharply pronounced resemblance to that of soils in areas treated with "Agent Orange" during the war [20]. This suggests that the transfer into the bay of at least part of the dioxins occurred via river run-off from the defoliant-treated areas.

It is very likely that over a relatively short period of time (2–3 years) after the massive treatments of the jungles were stopped considerable amounts of dioxin-containing defoliants, which were sprayed over the extensive watershed of the Kay River, were transferred via river run-off into the sea. Little-soluble and adsorbed components of toxicants together with bottom silts were subsequently redistributed over the bay. The toxic action of dioxin-containing defoliants on marine organisms entailed the inhibition of primarily hermatypic photosynthetic organisms and aerobic heterotrophic bacteria, which are the main components of reef ecosystems maintaining their stability. The primary massive chemical action was aggravated due to the periodic (during the rainy seasons) input of defoliant components from the river valley and to increasing anthropogenic pressure. Thus, the state of the bottom environments and the near-shore bottom communities in Nha Trang Bay has deteriorated markedly. The results of our investigations suggest that the presence of residues of dioxin-containing ecotoxicants in the marine bottom sediments is evidently the major stress factor (along with significant anthropogenic pressure) for the modern near-shore communities of Southern Vietnam. The adverse effect of dioxin-containing ecotoxicants is aggravated by the periodic stirring-up of silts during the storms and generally increased turbidity of the water as the results of the reduced coverage by live corals, which are the natural biological filters in the near-shore tropical ecosystems.

ACKNOWLEDGMENTS

The authors are grateful to the administrative and scientific staff of the Leading and Maritime Departments of the Russian–Vietnamese Tropical Center (Russian Academy of Sciences), as well as to the administrative and scientific staff of the Institute of Oceanography (National Center for Scientific Research of Vietnam in Nha Trang) for useful help in organization and provision for the fieldwork.

REFERENCES

1. Voronova, E.N., Volkova, E.V., Kazimirko, Yu.V., *et al.*, Measurements of the Cell's Photosynthetic Apparatus of the Diatom *Thallassiosira weissflogii* in Response to High Light Intensity, *Fiziol. Rast.*, 2002, vol. 49, no. 3, pp. 350–359.
2. Danilov, V.S. and Egorov, N.S., *Bakterial'naya biolyuminestsentsiya* (Bacterial Bioluminescence), Moscow: Mosk. Gos. Univ., 1985.
3. Klyuev, N.A., Dioxins—Supertoxicants of XXI Century. Problems, *Informatsionnyi vypusk*, no. 1 (News Letters. State Committee of Russian Federation for Environmental Protection), Moscow: VINITI, 1997, pp. 84–101.

4. Latypov, Yu.Ya., Composition and Distribution of Scleractinians on the Reefs of the Phukhanh Province (South Vietnam), *Biol. Morya*, 1982, no. 6, pp. 3– 12.
5. Latypov, Yu.Ya., Scleractinian Corals of Southern Vietnam, *Biol. Morya*, 1987, no. 5, pp. 12–19.
6. Latypov, Yu.Ya., *Korally skleraktinii Vietnama. Tamnasteriidy, Astrotseniidy, Potsilloporidy, Dendrofilliidy* (Scleractinian Corals of Vietnam. Tamnasteriidae, Astroceniidae, Pocilloporidae, Dendrophylliidae), Moscow: Nauka, 1990.
7. Latypov, Yu.Ya., *Korally skleraktinii Vietnama. Chast' II. Akroporidy* (Scleractinian Corals of Vietnam. Part II. Acroporida), Moscow: Nauka, 1992.
8. Latypov, Yu.Ya., *Korally skleraktinii Vietnama. Chast' III. Faviidy, Fungiidy* (Scleractinian Corals of Vietnam. Part III. Faviidae, Fungiidae), Moscow: Nauka, 1995.
9. Latypov, Yu.Ya. and Dautova, T.N., *Korally skleraktinii Vietnama. Chast' IV. Poritidy, Dendrofilliidy* (Scleractinian Corals of Vietnam. Part IV. Poritidae, Dendrophylliidae), Moscow: Nauka, 1996.
10. Matorin, D.N. and Venediktov, P.S., Luminescence of Chlorophyll in Microalgae Cultures and Natural Populations of Phytoplankton, *Itogi Nauki i Tekhn. VINITI. Ser. Biofiz.*, 1990, vol. 40, pp. 49–100.
11. *Opredelenie obshchei toksichnosti pochv po intensivnosti biolyuminestsentsii bakterii: Metodicheskie rekomendatsii* (Determination of General Toxicity of Soils by Intensity of Bacterial Bioluminescence: Methodical Recommendations), Moscow: Federal Center of State Sanitary and Epidemiological Inspection of Ministry of Health of Russia, 2000.
12. *Rukovodstvo po ekspluatatsii pribora biologicheskogo kontrolya "Biotoks- 10. Redaktsiya 2. IAYaK 4431-0017-05758078-00 RE. M."* (A Biological Control Device "Biotox-10." Operating Manual, Version 2), "Electrozavod" Holding Company, 2001.
13. Smurov, A.V., The State and Prospects for Recovery of Near-Shore Reefs of Nha Trang Bay (Southern Vietnam), *Tezisy 4 nauchn. konf. BBS MGU* (Abstracts of 4th Sci. Conf. of White Sea Biological Station of Moscow University, 10–11 August 1999, Moscow: Russkii Univ. 1999, pp. 54–56.
14. Smurov, A.V., Biological Methods for Diagnostic of Natural Environment, *Ekologicheskaya diagnostika. Seriya "Bezopasnost' Rossii"* (Ecological Diagnostic, Safety in Russia Series, MGF "Znanie," Moscow: Mashinostroenie. 2000, pp. 391–405.
15. Sorokin, Yu.I., *Ekosistemy korallovykh rifov* (Ecosystems of Corals Reefs), Moscow: Nauka, 1990.
16. Titlyanov, E.A., *Zooksantelly v germatipnykh korallakh: zhiznennaya strategiya* (Zooxanthellae in Hermatypic Corals: Life Stretegy), Vladivostok: Dalnauka, 1999.
17. Fonshtein, L.M., Kalinina, L.M., Polyushina, G.N., *et al.*, *Test-sistemy dlya otsenki mutagennoi aktivnosti zagryaznitelei v okruzhayushchei srede* (Test Systems for Evaluating Mutagenic Activity of Pollutants in the Environment), Moscow: Nauka, 1977.
18. Khudolei, V.V., Gusarov, E.E., Klinsky, A.V., *et al.*, *Stoikie organicheskie zagryazniteli: puti resheniya problemy* (Persistent Organic Pollutants: Ways for Solving the Problem), St.-Petersburg: Nauch.-Issled. Inst. Khim.; St. Peterb. Gos. Univ., 2002.
19. Davydoff, C.M., Contribution à l'ètude des invertébrés de la fauna marine bentique de l'Indochine, *Bull. Biol. France Belg.*, 1952, no. 32, Suppl., pp. 1– 158.
20. Kluyev, N.A., Cheleptchikov, A.A., Feshin, D.B., *et al.*, Vertical Migration of PCDD/F in Vietnamese Soils, *Organohalogen Comp.*, 2002, vol. 58, pp. 85–88.
21. Kotelevtsev, S.V., Stepanova, L.I., and Glaser, V.M., Biomonitoring of Genotoxicity in Coastal Waters, *Biomonitoring of Coastal Waters and Estuaries*, Boca Raton; Ann Arbor: CRC Press. 1994, pp. 227–247.
22. Lesser, M.P., Oxidative Stress Causes Coral Bleaching during Exposure to Elevated Temperatures, *Coral Reefs*, 1997, vol. 6, pp. 187–192.
23. Loi, T.N., Peuplements animaux et végétaux du substrat des intertidal de La Baine de Nha Trang (Viet Nam). Nha Trang. 1967.
24. Sheppard, C.R.C., Coral Populations on Reef Slopes and Their Major Controls, *Mar. Ecol. Prog. Ser.*, 1982, vol. 7, pp. 83–115.
25. Smith, S.V., Buddemeier, R.V., Global Change and Coral Reef Ecosystems, *Ann. Rev. Syst.*, 1992, vol. 23, pp. 89–118.
26. Titlyanov, E.A., Titlyanova, T.V., Leletkin, V.A., *et al.*, Degradation and Regulation of Zooxanthellae Density in Hermatypic Corals, *Mar. Ecol. Prog. Ser.*, 1996, vol. 139, pp. 167–178.

Australian Government
Department of Veterans' Affairs
Australian Institue of
Health and Welfare

Cancer Incidence

in Australian Vietnam Veterans

Study 2005

Executive Summary

Study initiation

A key recommendation of the 1997 *Mortality of Vietnam Veterans: The Veteran Cohort Study* was to monitor the mortality of Vietnam veterans and repeat the study after 2000. In 2002, the then Minister for Veterans' Affairs agreed that the Repatriation Commission should undertake the *Third Vietnam Veterans Mortality Study* and *Cancer Incidence in Vietnam Veterans Study*. The Commission asked the Australian Government Department of Veterans' Affairs (DVA) to conduct these studies which were undertaken with assistance from the Australian Institute of Health and Welfare (AIHW).

This report is the first of four volumes to be published and is the first investigation of cancer incidence for male Australian Vietnam veterans from all three branches of the armed forces – Navy, Army and Air Force. The number of females who served in Vietnam were too few for meaningful results in a study of this kind.

Study objectives

The objectives of the cancer incidence study were to:

- identify cases of cancer (excluding non-melanocytic skin cancers) among Vietnam veterans during the period 1982 to 2000 inclusive;
- compare the number of cases of cancer among Vietnam veterans with the number of expected cancers based on cancer incidence of the Australian community;
- report any differences in the cancer incidence for specific types of cancer, as highlighted by past studies and the literature review, from the Australian community;
- investigate any differences in cancer incidence between Navy, Army and Air Force Vietnam veterans;
- investigate any relationship between cancer incidence and exposure of Navy veterans to Vietnamese waters; and
- establish lists of personnel who served onboard HMA ships and Army small ships deployed to Vietnam and determine cancer incidence on a ship-by-ship basis.

Study design

The cancer incidence study is a retrospective cohort study of male Australian personnel who served in Vietnam between 23 May 1962 and 1 July 1973. The study examines cancers diagnosed during the period from 1982 to 31 December 2000. The study compares the cancer incidence rates of male Australian Vietnam veterans with those of Australian males in the general community. All comparisons have been standardised by age and year of diagnosis. In addition, the study analyses whether cancer incidence rates vary between different groups of Vietnam veterans or by duration of service in Vietnamese waters.

Report structure

Chapter One provides a background to previous studies and an overview of the study. **Chapter Two** of this Report provides a brief summary of the Vietnam War and Australia's involvement, which was formally announced in May 1962. There was a gradual build up of numbers, peaking in 1968, followed by a gradual decline until most of the troops had departed by the end of 1972.

The roll compiled for this study was drawn from the Nominal Roll of Vietnam Veterans currently maintained by DVA, as described in **Chapter Three**. The Nominal Roll has been extensively updated since it was last published in 1997. The Study Roll is a list of all those male defence personnel currently identified as serving in Vietnam between May 1962 and July 1973. The Study Roll contains a total of 59,179 Vietnam veterans.

The methodology for this study is outlined in **Chapter Four**. In brief, the Study Roll was matched against a number of databases, allowing determination of vital status (that is, whether a person is alive or dead), and determining the number of cancers. Vital status was determined for 97.5% of the cohort and 2.5% were lost to follow up. The number of cancers observed amongst the Vietnam veterans was compared to the number expected in Australian men of the same age.

As outlined in **Chapter Five**, the nature of service varied considerably between the Service branches. Army and Air Force veterans averaged approximately one year of service in Vietnam whereas Navy veterans averaged approximately three months. The Navy personnel were substantially younger than the Army or Air Force personnel when they first served in Vietnam.

The results of the cancer incidence analysis are presented in **Chapter Six** and these findings are discussed in **Chapter Seven**.

Findings

The results presented in **Chapter Six** show that Australian Vietnam veterans have a significantly elevated overall cancer incidence rate that is 13-15% higher than expected.

Incidence rates for specific cancers of *a priori* interest showed a mixed pattern. Rates of five cancers (head and neck, lung, prostate, Hodgkin's disease and melanoma) were significantly higher than expected. Four cancers (liver, thyroid, multiple myeloma and non-Hodgkin's lymphoma) showed a significantly lower cancer rate than expected.

The pattern of cancer incidence varied between the Service branches. Navy veterans had the highest rate of cancer, higher than expected by 22-26%, followed by Army veterans, higher than expected by 11-13%. In comparison Air Force veterans had a 6-8% higher than the expected rate of cancer, although this was not statistically significant.

Veterans from all Service branches showed a higher than expected incidence of genitourinary cancers and melanoma. Navy and Army veterans showed a higher than the expected incidence of cancers of the lung, oral cavity, pharynx and larynx and cancers of the head and neck. Whereas Navy veterans demonstrated a higher than the expected incidence of gastrointestinal cancer, Army and Air Force veterans showed higher than the expected incidence of Hodgkin's disease and prostate cancer. It should be noted that veterans from all three Service branches showed lower than the expected incidence of non-Hodgkin's lymphoma.

An exposure of particular interest to Vietnam veterans is the herbicides that were used in Vietnam. The rate for several of the cancers that have been associated with herbicide exposure are high in this study; several others do not differ from expectation; others are significantly below the community norm.

Within the limitations of the service details available for Navy personnel, the higher than expected cancer incidence among this group could not be attributed to either the ship on which they served or the time spent in Vietnamese waters.

Strengths and Weaknesses of the Study

As discussed in **Chapter Seven**, the strengths of the study include its size, data quality, high percentage of known vital status, homogeneity of the study population, extensive consultation with the veteran community and close external scientific advice.

The study had limited ability to quantify exposures, making it difficult to assign any observed outcome to a particular exposure. A discussion of the possible exposures that could be an explanation of the observed pattern of cancer is contained within this Report, but, given the uncertainties associated with exposure, this discussion is, by necessity, speculative in nature.

Conclusion

In conclusion, this study provides good evidence that Australian male veterans of the Vietnam War have an increased rate of cancer overall. There was an excess of 613 cancers; 88% of this excess consisted of lung cancers, oral cavity, pharynx and larynx cancers, prostate cancers and melanomas. The pattern is not generally consistent across the Navy, Army and Air Force veterans, although melanoma, and to a lesser degree prostate cancer, were consistently elevated in all three groups.

Additional Work

Three more reports will be completed in this series during 2005. The second volume will be a mortality study of all male Vietnam veterans. The third volume will investigate the mortality and cancer incidence of national service veterans and non-veterans. Finally the fourth volume will repeat the 1992 Dapsone study to investigate the effect of exposure to this anti-malarial drug on mortality and cancer incidence among the male Army cohort.

This further research may enable more useful observations to be made about the health of Vietnam veterans.